ENGINEERING TRANSACTIONS • *Engng. Trans.* • **50**, 3, 107–164, 2002
Polish Academy of Sciences • Institute of Fundamental Technological Research
10.24423/engtrans.517.2002

THERMODYNAMICAL THEORY OF INELASTIC SINGLE CRYSTALS

Piotr Perzyna

Institute of Fundamental Technological Research,
Polish Academy of Sciences,
Świętokrzyska 21, 00-049 Warsaw, Poland

The paper aims at the development of the thermodynamic theory of elasto-viscoplasticity of single crystals which takes account of the evolution of the dislocation substructure. The next objective is the application of the theory developed for the investigation of the adiabatic shear-band formation in single crystals under dynamic loading processes. The description of the kinematics of finite elasto-viscoplastic deformations of single crystal is based on notions of the Riemannian space of manifolds and the tangent space. A multiplicative decomposition of the deformation gradient is adopted and the Lie derivative is used to define all objective rates for the introduced vectors and tensors. A general constitutive model is developed within the thermodynamic framework of the rate-type covariance constitutive structure with finite set of the internal state variables, and takes account of the effects as follows: (i) thermomechanical coupling; (ii) influence of covariance terms, lattice deformations and rotations and plastic spin; (iii) evolution of the dislocation substructure; (iv) deviation from the Schmid rule of a critical resolved shear stress for slip; (v) rate sensitivity (viscosity). A notion of covariance is understood in the sense of invariance under arbitrary spatial diffeomorphisms. The developed thermoviscoplasticity theory of single crystals is based on the axioms as follows: (i) existence of the free energy function; (ii) invariance with respect to any diffeomorphism (any superposed motion); (iii) assumption of the entropy production inequality; (iv) assumption of the evolution equations for the internal state variables in the particular rate-dependent form. To describe the evolution of the dislocation substructure, a finite set of the internal state variables is interpreted as follows: the density of mobile dislocations, the density of obstacle dislocations and the concentration of the point defects. Physical foundations and experimental motivations are given. Two fundamental constitutive equations of the rate-type for the Kirchhoff stress tensor and temperature are formulated. To show that the thermodynamic theory of viscoplasticity of single crystals takes account of all the mentioned effects, an analysis of the thermomechanical couplings and internal dissipation is presented. Particular attention is focused on synergetic effects, generated by cooperative phenomena of thermomechanical couplings and the influence of the evolution of the dislocation substructure. The initial boundary value problem (the evolution problem) for rate-dependent elasto-plastic single crystal has been proved to be well posed. Criteria for adiabatic shear-band localization of plastic deformation are obtained by assuming that some eigenvalue of the instantaneous adiabatic acoustic tensor for rate-independent response is equal to zero. The formation of the adiabatic shear-band is investigated. It has been found that the synergetic effects generated by cooperative phenomena of thermomechanical couplings and the influence of the evolution of the dislocation substructure play a fundamental role in the inception of localization. The results obtained are compared with available experimental observations.

1. Introduction

Recent experimental observations and theoretical investigations have shown that the synergetic effects have a great influence on the behaviour of inelastic single crystals. Particularly, the adiabatic shear-band localization in single crystals is affected very much by cooperative phenomena.

Experimental observations of the macroscopic adiabatic shear-band localization in single crystals performed by CHANG and ASARO [7, 8], SPITZIG [64] and LISIECKI *et al.* [35] showed that the strain-hardening rate h_{crit} at the inception of shear-band localization is positive and the direction of the localized shear-band is misaligned by some small angle δ from the active slip system.

On the other hand, the investigations presented by MECKING and KOCKS [39], FOLLANSBEE [19] and FOLLANSBEE and KOCKS [20] showed a great influence of the strain-rate sensitivity on the behaviour of inelastic metallic single crystals in dynamic loading processes. To describe the strain-rate sensitivity effects, FOLLANSBEE [19] suggested to take into consideration the evolution of the dislocation substructure.

Experimental study of highly heterogeneous deformations in copper single crystals performed by RASHID *et al.* [57] showed that the strain-rate history dependence of the substructure evolution plays an important role, particularly in adiabatic shear-band formation phenomena.

ASARO and RICE [3] have clearly shown that the classical theory of crystals based on the Schmid constitutive law does not seem to be appropriate to explain the shear-band localization phenomenon in ductile metallic single crystals.

ASARO and RICE [3] have focused attention on the localization criteria for "an assumed class of materials that essentially obey Schmid's rule but display modest departure from it". They proved that the plastic hardening rate h_{crit} at the inception of localization may be positive when there are deviations from the Schmid law, cf. also QIN and BASSANI [55, 56] and BASSANI [6].

To describe the main experimentally observed facts connected with the macroscopic shear-band formation, DUSZEK-PERZYNA and PERZYNA [14] have considered the synergetic effects resulting from taking into account spatial covariance effects and thermomechanical couplings. PERZYNA and KORBEL [53] have investigated the influence of the evolution of substructure on the shear-band localization phenomena in single crystals for single slip process. DUSZEK-PERZYNA and PERZYNA [15] have examined the influence of thermal expansion, thermal plastic softening and spatial covariance effects on shear-band localization criteria for a planar model of an f.c.c. crystal undergoing symmetric primary-conjugate double slip process, cf. also PERZYNA and DUSZEK-PERZYNA [52]. In the paper by PERZYNA and KORBEL [54], the attention is focused on the discussion of the cooperative influence of various effects on the criteria for shear-band localization

in both the symmetric double slip and single slip processes.

It has been proved by the previously mentioned theoretical investigations that the main cooperative phenomena which affect the behaviour of metallic single crystals are generated by thermomechanical couplings and the evolution of the dislocation substructure.

To describe the influence of main cooperative phenomena on the behaviour of metallic single crystals, we intend to start from the development of the thermodynamic theory of single crystals with special emphasis on the investigations of thermomechanical couplings and internal dissipative effects. Then this theory is used for the investigations of the adiabatic shear-band formation in single crystals under dynamic loading processes.

In Section 2 the experimental observations of shear-band localization in single crystals are discussed. Particular attention is focused on the experimental motivations of the influence of the evolution of the substructure on the behaviour of single crystals in the critical situation when the macroscopic localized shear-band is formed. Physical motivations of the new thermodynamic viscoplasticity theory of metallic single crystals have been presented. The discussion of various physical mechanisms of dislocation motion, and particularly the interaction of the thermally activated and phonon damping mechanisms has been given. The relaxation time treated as a microstructural parameter has been introduced. It has been shown that the proposed viscoplastic model accomplishes the description of behaviour of single crystals valid for the entire range of strain-rate changes and encompasses the interaction of the thermally activated and phonon damping mechanisms.

In Section 3 the kinematics of finite elasto-viscoplastic deformations of single crystals are presented. The description is based on notions of the Riemannien space on manifolds and the tangent space. A multiplicative decomposition of the deformation gradient is adopted and the Lie derivative is used to define all objective rates for the introduced vectors and tensors. Fundamental definitions of stress tensors and the resolved Schmid stress are introduced.

Section 4 is devoted to the development of a rate-dependent constitutive model of inelastic single crystal within the thermodynamic framework of the rate-type covariance constitutive structure with internal state variables. It has been assumed that a set of the internal state variables consists of the shearings $\gamma^{(\nu)}$, the densities of mobile dislocations $\alpha^{(\nu)}$, the densities of obstacle dislocations $\beta^{(\nu)}$ and the concentrations of point defects $\xi^{(\nu)}$ $(\nu = 1, 2, \ldots, n)$. The development of the constitutive structure is based on the four axioms, namely the existence of the free energy function, the spatial covariance objectivity, the entropy production postulate and the assumption of the evolution equations for the internal state variables. The fundamental rate-type constitutive equations for the Kirchhoff stress tensor $\boldsymbol{\tau}$ and for temperature ϑ are formulated. Thermome-

chanical couplings are investigated. The description of internal heating generated by the rate of internal dissipation is presented.

In Section 5 a rate-independent response of elasto-plastic single crystal is investigated as a particular case of general rate-dependent constitutive structure.

Section 6 is devoted to the formulation of an adiabatic process. Discussion of cooperative phenomena is presented. The rate of stored energy is defined. It has been shown that the stored energy is attributed to the evolution of the dislocation substructure. Mathematical description of both rate-dependent and rate-independent adiabatic processes is given.

Section 7 is focused on an analysis of acceleration waves. It has been proved that in an adiabatic process for both elastic-viscoplastic and elastic-plastic rate-independent model of single crystal, the acceleration discontinuity $[\![\mathbf{a}]\!]$ is the solution of the appropriate eigenvalue problem. In these eigenvalue problems, the instantaneous adiabatic acoustic tensors $\mathbf{A}$ and $\hat{\mathbf{A}}$ play a fundamental role.

In Section 8 the macroscopic shear-band formation during an adiabatic process for symmetric double slip and single slip in elastic-plastic rate-independent single crystal are studied. The necessary condition for a localized plastic deformation region to be formed is obtained when the determinant of the instantaneous acoustic tensor $\hat{\mathbf{A}}$ is equalled to zero. The criteria for adiabatic shear-band localization in the single slip process are obtained in exact analytical form. For the symmetric double slip process these criteria have been estimated numerically. The identification procedure for material constants has been presented. Numerical estimations for the critical hardening modulus rate h_{crit} and the direction of the macroscopic shear-band are given. An analysis of the influence of various effects on shear-band localization criteria is presented. Particular attention is focused on the investigation of the influence of the evolution of the substructure and thermomechanical couplings.

Section 9 is devoted to the discussion of the results obtained. Comparison of the numerical results with available experimental data is presented. The possibility of deviations from the Schmid rule of the critical resolved shear stress is also investigated. The critical value of the hardening modulus rate h_{crit} predicted by the theory for a single slip process is in accord with experimental observations, while the misalignment of the shear-bands from the active slip systems in the crystal matrix is too small. For symmetric double slip process, both the values obtained are in accord with experimental observations. It has been found that the influence of the dislocation substructure is combined with the thermomechanical couplings, and that is why it gives a distinct synergetic effect.

Section 10 is devoted to final comments. Main features of the developed thermodynamic theory of single crystals are discussed. It has been emphasized that application of this theory to the adiabatic shear-band formation has proved the importance of the influence of cooperative phenomena and synergetic effects.

2. Experimental and physical foundations

2.1. Experimental observations of single crystal behaviour

The high-rate deformation of face-centered cubic (f.c.c.) metals, such as copper, aluminum, lead and nickel has been recently extensively studied (cf. the review paper by FOLLANSBEE [19]). It has been shown that the apparent strain-rate sensitivity of f.c.c. metals has two origins: that associated with the finite velocity of dislocations, and that connected with the evolution of the dislocation substructure. The first of these two components – the instantaneous rate sensitivity – is related to the wait – times associated with thermally activated dislocation motion. The second component has more to do with the relative importance of dislocation generation and annihilation at different strain-rates, and shall be referred to as the strain-rate history effect.

RASHID *et al.* [57] performed an experimental study of highly heterogeneous deformations in copper single crystals to investigate the importance of the dislocation substructure. Their experimental results are mainly qualitative in nature, and include optical photographs and micrographs of the deformed specimens, and scanning and transmission electromicrographs of the substructure. The results obtained seem to support the earlier findings related to the strain-rate history dependence of the substructure evolution. The higher total dislocation density observed in the notch region of the dynamically deformed specimen, as compared to the same region in the quasi-statically deformed specimen, reflects the higher shear stress attained in the dynamic case, cf. Figs. 1 and 2.

When ductile single crystals of metals are finitely deformed, they display highly heterogeneous deformation, e.g. when crystals are stretched in tension, they can neck and then develop macroscopic bands of localized shearing.

Experimental observations of CHANG and ASARO [7, 8], LISIECKI *et al.* [35] and SPITZIG [64] for copper, aluminum – copper and nitrogenated Fe-Ti-Mn single crystals investigated in uniaxial tension tests have shown that in the first stage of the process, a crystal specimen undergoes uniform extension in single slip. At the point when the load-engineering strain trajectory reaches its maximum, a crystal specimen exhibits slight amounts of very diffuse necking, cf. Figs. 3, 4 and 5. The neck is usually symmetric in shape indicating that double slip is operative within it, cf. LISIECKI *et al.* [35]. At this stage of the tensile process, the gross plastic deformations are localized to the diffusely necked region and the thermomechanical coupling effects begin to play a crucial role. That is why in this region of the specimen the tensile process has to be considered as adiabatic. With continued extension the macroscopic, adiabatic shear-bands have soon developed within the diffusely necked region. This point on the shear stress – shear strain trajectory is found experimentally to lie on the increasing

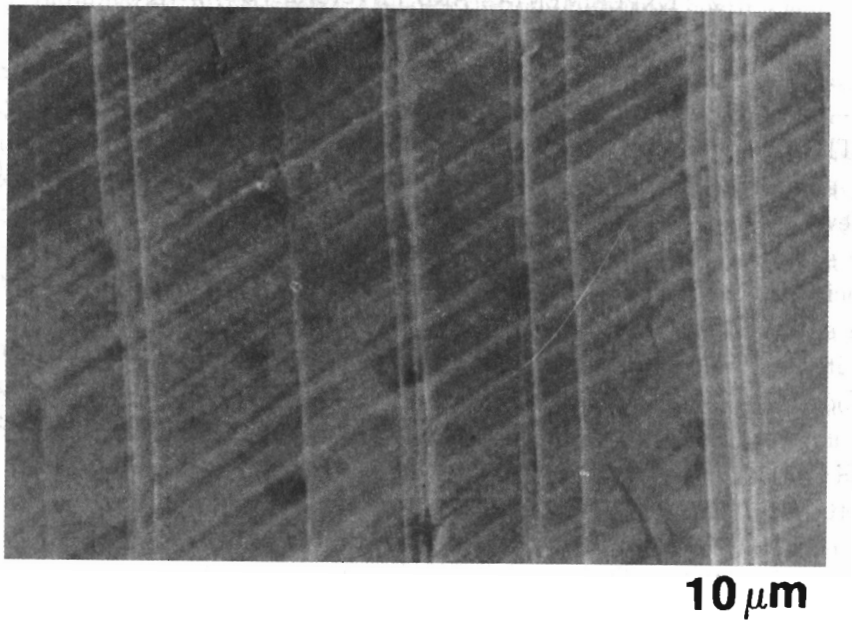

FIG. 1. Scanning electron micrograph of an intensely deformed region of a dynamically deformed specimen, taken to the left of the specimen centreline. The lattice rotation is clearly evident (after RASHID *et al.* [57]).

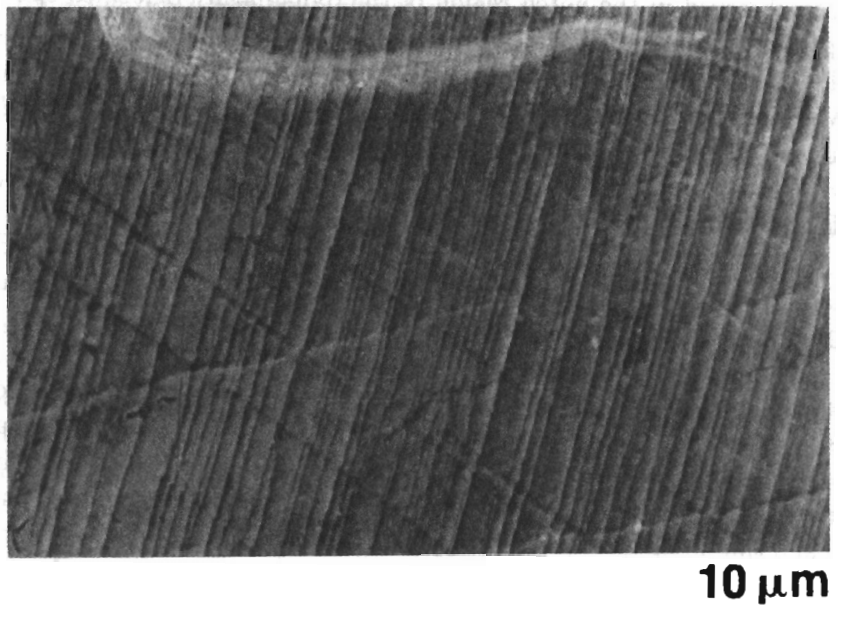

FIG. 2. Scanning electron micrograph taken near the right corner of the indenter notch on the quasi-statically deformed specimen (after RASHID *et al.* [57]).

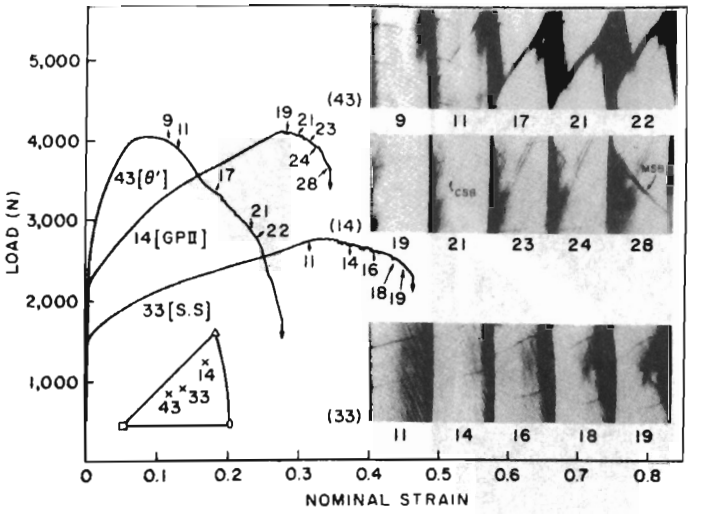

FIG. 3. Load versus engineering strain curves for various ageing treatments. Numbered photos correspond to the indicated points on the load-strain curves (after CHANG and ASARO [8]).

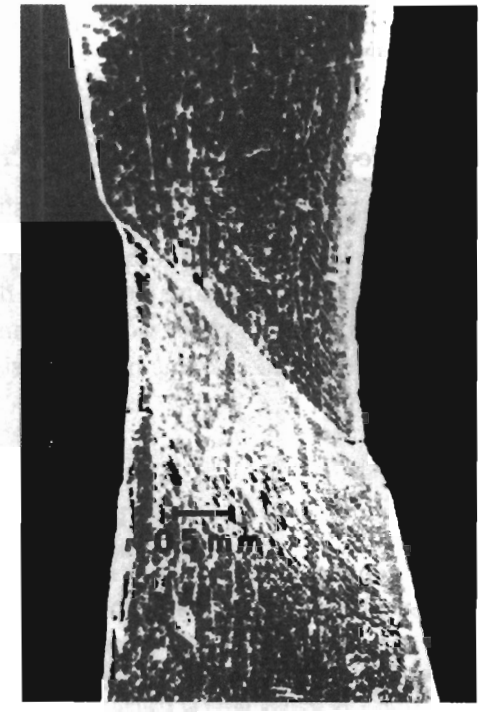

FIG. 4. Single crystal of aluminum – 2.8 wt. percent copper deformed in tension (after LISIECKI *et al.* [35]).

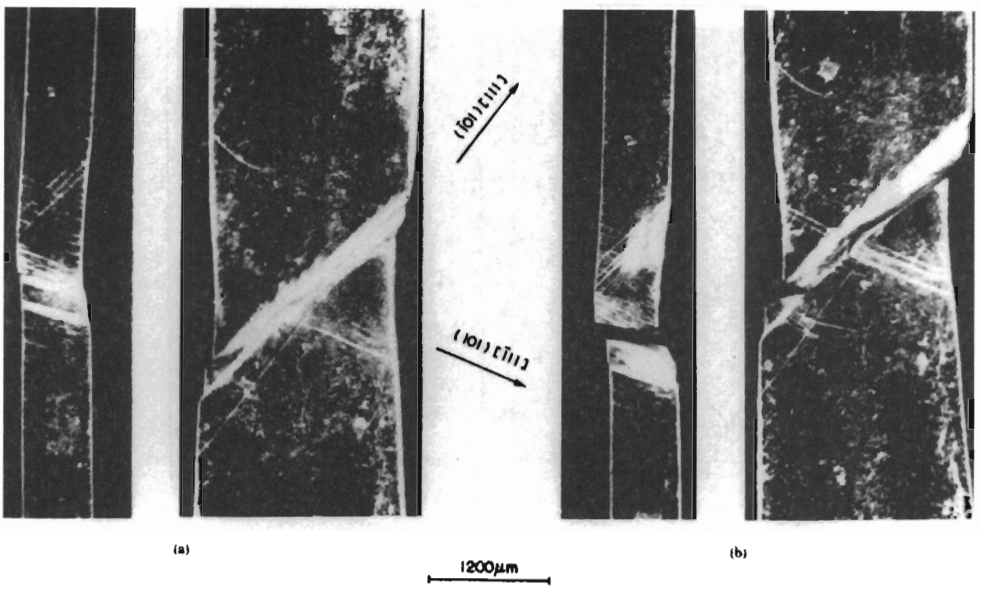

FIG. 5. Propagation of localized shear-band in nitrogenated Fe-Ti-Mn crystal deformed at 295 K: (a) 20 percent decrease in load maximum load, (b) 40 percent decrease in load maximum load (after SPITZIG [64]).

part of this curve very near to the maximum point, so that a critical value of the strain-hardening modulus rate $h_{\text{crit}} = \left(\frac{d\tau}{d\gamma}\right)$ is small but positive, cf. Fig. 6.

It has been experimentally observed that at the inception of the macroscopic, adiabatic shear-band, the direction of the band is slightly different from the detected coarse slip bands or slip traces. In other words, the macroscopic shear-bands are not aligned with the active slip systems in the crystal matrix but are misaligned by angle δ, cf. Figs. 7 and 8.

2.2. Dynamic behaviour of crystals

The rate and temperature dependence of the flow stress of metal crystals can be explained by different physical mechanisms of dislocation motion. The microscopic processes combine in various ways to give several groups of deformation mechanisms, each of which can be limited to the particular range of temperature and strain-rate changes.

It will be profitable for further considerations to discuss some of these mechanisms, particularly those which lead to viscoplastic response of the crystal.

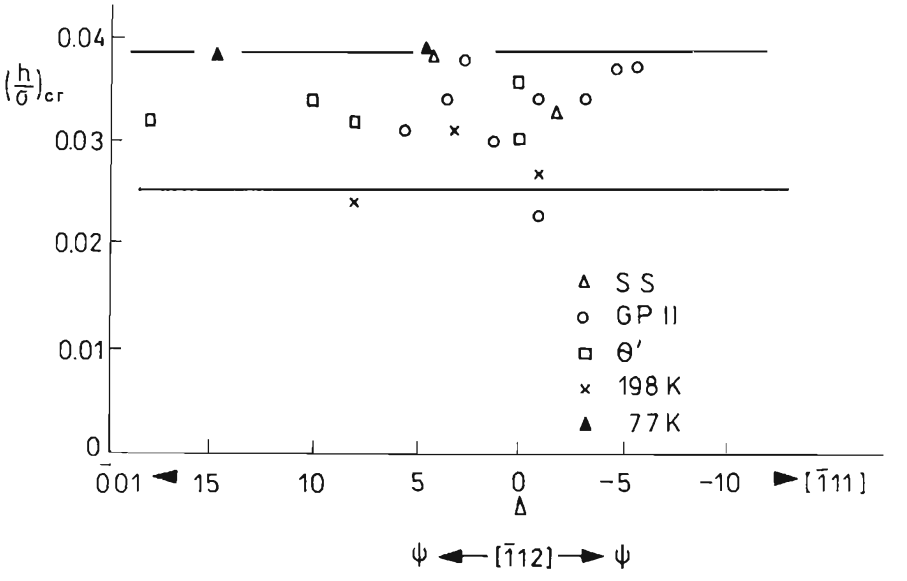

FIG. 6. Critical ratio $(h/\sigma)_{\text{crit}}$ versus ψ, the angle between the tensile axis and $[\bar{1}12]$ for various ageing treatments (after CHANG and ASARO [8]).

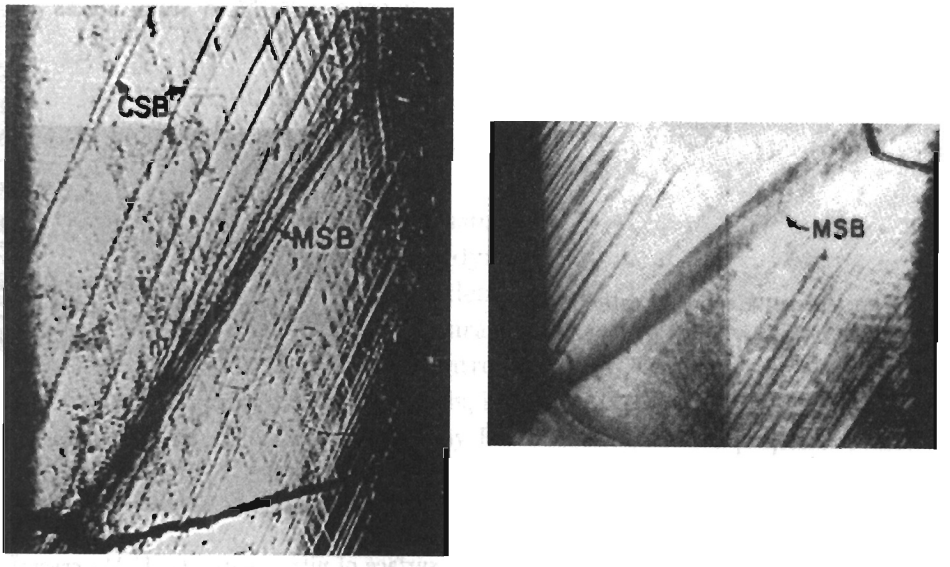

FIG. 7. Coarse slip band (CSB) and macroscopic shear-bands (MSB) in (a) GPII tested at 77 K and (b) a θ' strengthened crystal tested at 298 K. Note the orientation difference between CSBs and MSBs in (a), CSBs are closely aligned with the active slip systems (after CHANG and ASARO [8]).

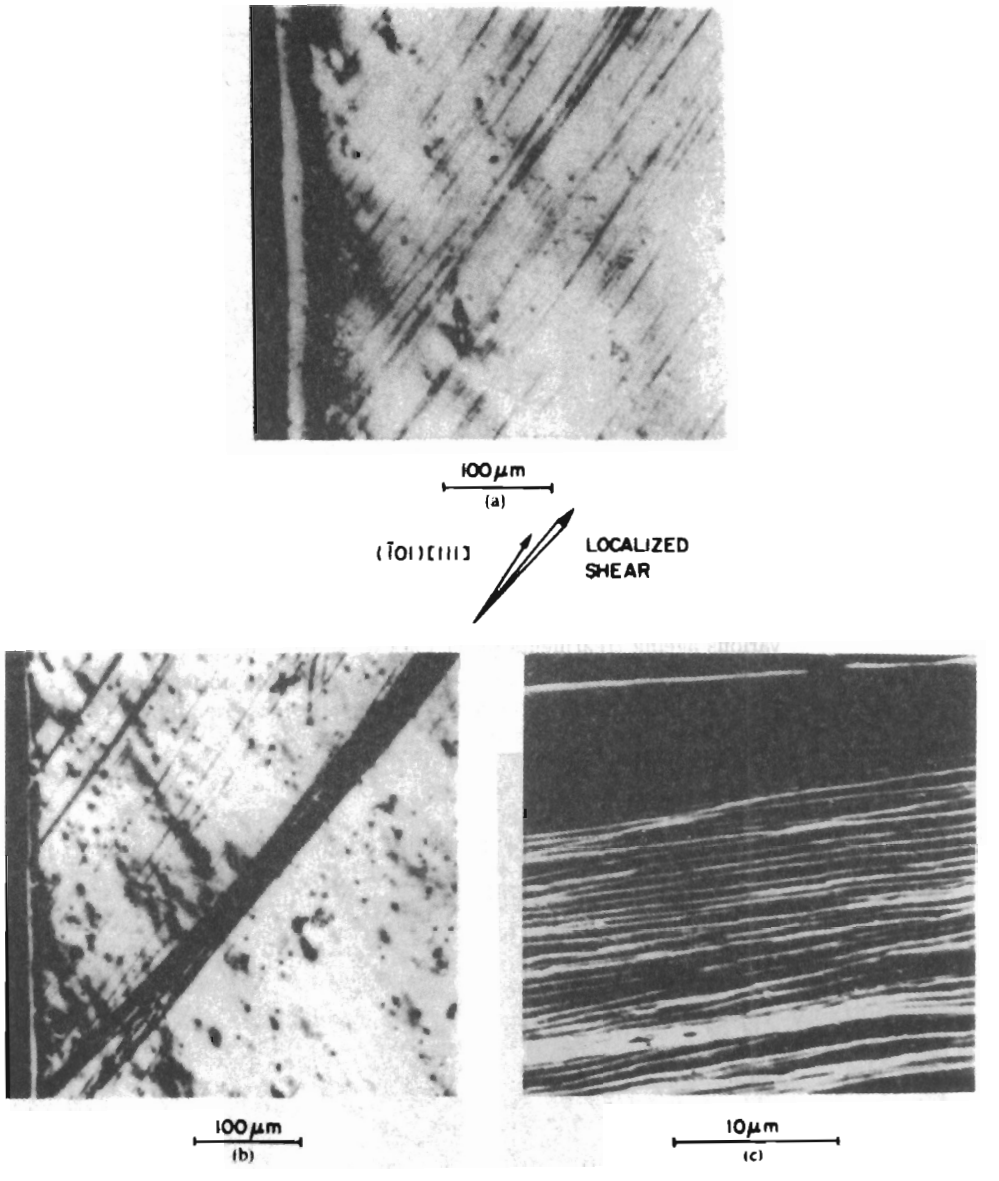

FIG. 8. Slip traces and localized shear on the surface of nitrogenated Fe-Ti-Mn crystal of orientation D deformed at 295 K: (a) initial deformation until necking began, (b) subsequent deformation after removal of neck and localized shear-bands from initial deformation, (c) slip traces within localized shear-band in (b) (after SPITZIG [8]).

Some common thermal obstacles or mechanisms in pure metals are as follows: (i) intersection of forest dislocations; (ii) overcoming Peierls-Nabarro stress; (iii) non-conservative motion of jogs; (iv) cross-slip of screw dislocations; (v) climb of edge dislocations. Forest dislocations, the Peierls-Nabarro stress and jogs represent resistance to the motion of dislocations in the slip plane, while cross-slip and climb represent resistance to the motion out of the slip plane. Schematic representations of the ways in which these obstacles are overcome are given in Fig. 9. In each case, thermal fluctuations assist the applied stress in getting a dislocation segment L past the barrier (cf. CONRAD [11]).

To describe theoretically all the mechanisms we have to introduce three important parameters, namely the density of mobile dislocations α, the density of obstacle dislocations β and the concentration of point defects ξ. Average density of mobile dislocations in deformed metal single crystals is of the order of $10^{15}\mathrm{m}^{-2}$, average density of obstacle dislocations is $10^{13}\mathrm{m}^{-2}$, and the average value of the concentration of point defects can be of the order of $10^{15}\mathrm{m}^{-3}$.

Since plastic flow occurs by the motion of dislocation lines, the rate at which it takes place depends on how fast the dislocations move, how many dislocations are moving in a given volume of material, and how much displacement is carried by each dislocation. The theory of crystal dislocations shows that for the single slip, the inelastic shear strain-rate is as follows

$$\dot{\epsilon}^p = \alpha b \mathrm{v}, \tag{2.1}$$

where α is the mean density of mobile dislocations, b is the displacement per dislocation line (the Burgers vector), and v denotes the mean dislocation velocity.

2.2.1. Thermally activated mechanism. It is now generally recognized that the plastic deformation of a crystal is of dynamic nature and has been established as a thermally activated process dependent upon time, temperature and strain-rate. The evolution of the activation parameters is a widely used technique for the identification of the mechanisms controlling the rate of deformation, and has been applied to b.c.c., f.c.c., h.c.p. metals, intermetallic compounds and ionic and ceramic crystals (cf. the review paper by Evans and KUMBLE [18] and books by NABARRO [42], and KOCKS *et al.* [33]).

When a dislocation moves through a crystal lattice, a force is exerted upon it by obstacles present in the lattice. This force can be separated into two components, a long-range force and short-range force.

The stress nesessary to overcome the short-range obstacles is temperature-dependent, whereas that needed to surmount fixed long-range obstacles generally depends upon temperature only through the temperature-dependence of the shear modulus. For this reason the obstacles are often referred to as thermal and

(i) INTERSECTION OF FOREST DISLOCATIONS

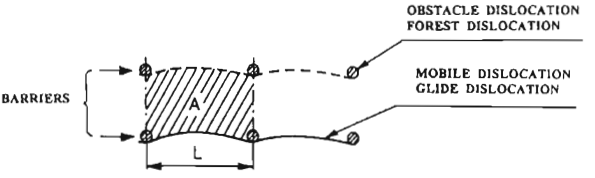

(ii) OVERCOMING PEIERLS-NABARRO STRESS

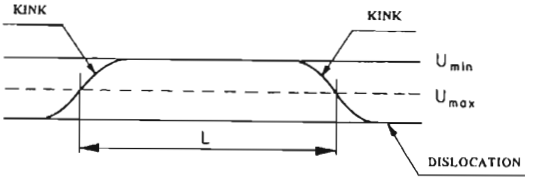

(iii) NON-CONSERVATIVE MOTION OF JOGS

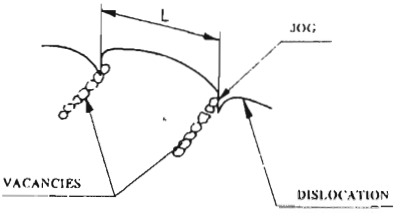

(iv) CROSS-SLIP

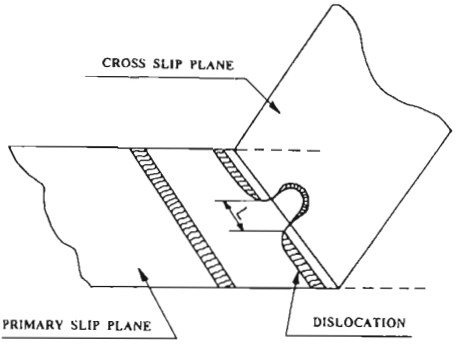

(v) CLIMB

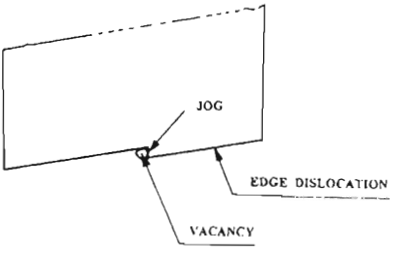

α DENSITY OF MOBILE DISLOCATIONS (10^{14} m^{-1})
β DENSITY OF OBSTACLE DISLOCATIONS (10^{13} m^{-1})
ξ CONCENTRATION OF POINT DEFECTS (10^{13} m^{-3})

FIG. 9. Schematic representation of thermal obstacles or mechanisms in pure metals (cf. CONRAD [11]).

athermal, respectively. When both types of obstacles are present in a lattice, the applied stress is usually comprosed of both thermal and athermal components

$$\tau = \tau^{\#} + \tau_{\mu}, \tag{2.2}$$

where $\tau^{\#}$ is the thermal (or effective) resolved shear stress and τ_{μ} is the athermal stress.

Plastic deformation occurs by the movement of a large number of dislocations through an array of obstacles. At any finite temperature, coherent atomic fluctuations can assist the applied stress in moving a dislocation past the obstacles, cf. Fig. 9(i).

The average velocity v of a dislocation that surmounts the obstacles with the assistance of thermal fluctuations is assumed to be an Arrhenius-type relationship

$$\mathrm{v} = AL^{-1}\nu \exp\left(-\frac{U}{k\vartheta}\right), \tag{2.3}$$

where ν is the frequency of vibration of the dislocation, AL^{-1} is the distance covered after a successful fluctuation, U is the activation energy (Gibbs free energy), k is the Boltzmann constant and ϑ is actual absolute temperature.

Equations (2.1) and (2.3) give

$$\dot{\epsilon}^{p} = \alpha b A L^{-1} \nu \exp\left(-\frac{U}{k\vartheta}\right). \tag{2.4}$$

Let us assume that

$$U = U[(\tau - \tau_{\mu}) L b], \tag{2.5}$$

where L is the mean cord distance between the neighboring points at which the dislocation is arrested. Expansion of the function U gives

$$U = U\,|_{\tau=\tau_{\mu}} + U'\,|_{\tau=\tau_{\mu}}\,(\tau - \tau_{\mu}) L b + U''\,|_{\tau=\tau_{\mu}}\,\frac{(\tau - \tau_{\mu})^2 L^2 b^2}{2!} + \cdots \tag{2.6}$$

Let us denote by

$$v^{*} = -U'\,|_{\tau=\tau_{\mu}}\,Lb, \quad U_{\circ} = U\,|_{\tau=\tau_{\mu}}, \tag{2.7}$$

the activation volume and the activation energy for intersection at zero effective stress, respectively.

The linear approximation to Eq. (2.4) gives the SEEGER relation (cf. SEEGER [60, 61])

$$\dot{\epsilon}^{p} = \alpha b A L^{-1} \nu \exp\left\{-\frac{U_{\circ}}{k\vartheta} + \left[(\tau - \tau_{\mu})\frac{v^{*}}{k\vartheta}\right]\right\}, \tag{2.8}$$

or

$$\tau = \left(\tau_\mu + \frac{U_\circ}{v^*}\right) + \frac{k\vartheta}{v^*} \ln \frac{\dot{\epsilon}^p}{\alpha b A L^{-1} \nu}. \tag{2.9}$$

When the activation energy U is a nonlinear function of the effective stress (cf. Eq. (2.5)), the relation (2.4) yields

$$\dot{\epsilon}^p = \alpha b A L^{-1} \nu \exp\left\{-U\left[(\tau - \tau_\mu) Lb\right]/k\vartheta\right\} \tag{2.10}$$

or

$$\tau = \tau_\mu + \frac{1}{Lb} U^{-1}\left[k\vartheta \ln\left(\alpha b A L^{-1} \nu / \dot{\epsilon}^p\right)\right]. \tag{2.11}$$

Let us denote by

$$T_{mT} = \frac{1}{\gamma_T} = (\alpha b A L^{-1} \nu)^{-1}, \quad \tau_B = (\tau_\mu + U_\circ / v^*), \tag{2.12}$$

the relaxation time for the thermally activated mechanism of dislocation motion (γ_T defines the viscosity coefficient) and the flow stress τ_B, respectively. Then the relations (2.8) and (2.9) take the form

$$\dot{\epsilon}^p = \frac{1}{T_{mT}} \exp\left[\frac{v^*}{k\vartheta}(\tau - \tau_B)\right], \quad \tau = \tau_B + (k\vartheta/v^*) \ln(T_{mT} \dot{\epsilon}^p). \tag{2.13}$$

In this linear theory we have three intrinsic material parameters, namely the relaxation time T_{mT}, the activation volume v^* and the flow stress τ_B.

In the most general case, each of these three parameters may be considered as a function of the three independent variables ϵ^p, τ and ϑ.

In the nonlinear theory

$$\dot{\epsilon}^p = \frac{1}{T_{mT}} \exp\{-U[(\tau - \tau_\mu) Lb]/k\vartheta\} \tag{2.14}$$

or

$$\tau = \tau_\mu + \frac{1}{Lb} U^{-1}\left[k\vartheta \ln\left(\frac{1}{T_{mT} \dot{\epsilon}^p}\right)\right] \tag{2.15}$$

there are two intrinsic material parameters T_{mT} and τ_μ and, in addition, one response function U.

2.2.2. Damping mechanism (phonon viscosity). With increasing dislocation velocities at high enough stress or in a perfect crystal, the velocity is only governed by the phonon damping mechanism. The phonon viscosity theory has been developed by MASON [37] (cf. NABARRO [42]). At very high strain-rates, the applied stress is high enough to overcome instantaneously the dislocation barriers without any aid from thermal fluctuations. This is true for the resolved shear stress $\tau > \tau_B$, where τ_B is attributed to the stress needed to overcome the forest dislocation barriers to the dislocation motion and is called the back stress.

In this region of response, the evolution equation for the inelastic shearing has the form

$$\dot{\epsilon}^p = \frac{\alpha b^2 \tau_\mu}{B}\left[\frac{\tau}{\tau_B} - 1\right], \tag{2.16}$$

where B is called the dislocation drag coefficient. If we introduce the denotation

$$T_{mD} = \frac{B}{\alpha b^2 \tau_B} = \frac{1}{\gamma_D} \tag{2.17}$$

for the relaxation time for the phonon damping mechanism (γ_D defines the viscosity coefficient for this region), then the evolution equation (2.16) takes the form

$$\dot{\epsilon}^p = \frac{1}{T_{mD}}\left(\frac{\tau}{\tau_B} - 1\right) \tag{2.18}$$

or

$$\tau = \tau_B\,(1 + T_{mD}\dot{\epsilon}^p)\,. \tag{2.19}$$

For the phonon damping mechanism we have two intrinsic parameters, namely the relaxation time T_{mD} and the back stress. It is noteworthy that the dislocation drag coefficient B can be interpreted as a generalized damping parameter for phonon viscosity and electron viscosity mechanisms (cf. GORMAN *et al.* [22]) i.e.

$$B = B_{pv} + B_{ev}. \tag{2.20}$$

2.2.3. Interaction of the thermally activated and phonon damping mechanisms. If a dislocation is moving through the rows of barriers, then its velocity can be determined by the expression

$$\mathrm{v} = AL^{-1}/(t_S + t_B), \tag{2.21}$$

where AL^{-1} is the average distance of dislocation movement after each thermal activation, t_S is the time a dislocation spent at the obstacle, and t_B is the time of travelling between the barriers.

The shearing rate in single slip is given by the relationship (cf. KUMAR and KUMBLE [34], TEODOSIU and SIDOROFF [67] and PERZYNA [48, 49])

$$\dot{\epsilon}^p = \frac{1}{T_{mT}} \langle \exp\{U[(\tau - \tau_\mu)Lb]/k\vartheta\} + BAL^{-1}\nu/(\tau - \tau_B)b\rangle^{-1} \tag{2.22}$$

where

$$\frac{1}{T_{mT}} \frac{b\tau_B}{BAL^{-1}\nu} = \frac{\alpha b^2 \tau_B}{B} = \frac{1}{T_{mD}}, \tag{2.23}$$

and two effective resolved shear stresses

$$\tau_T^* = \tau - \tau_\mu \quad \text{and} \quad \tau_D^* = \tau - \tau_B \tag{2.24}$$

are separately defined for the thermally activated and phonon damping mechanisms, respectively.

If the time t_B taken by the dislocation to travel between the barriers in a viscous phonon medium is negligible when compared with the time t_S spent at the obstacle, then

$$\mathrm{v} = \frac{AL^{-1}}{t_S} \tag{2.25}$$

and we can focus our attention on the analysis of the thermally activated process.

When the ratio t_B/t_S increases then the dislocation velocity (2.21) can be approximated by the expression

$$\mathrm{v} = \frac{AL^{-1}}{t_B} \tag{2.26}$$

for the phonon damping mechanism.

2.3. Viscoplastic model of single crystals

The main idea of the viscoplastic flow mechanism is to accomplish in one model the description of behaviour of single crystals valid for the entire range of strain-rate changes. In other words, the main concept is to encompass the interaction of the thermally activated and phonon damping mechanisms.

To achieve this aim, the empirical overstress function Φ has been introduced and the strain-rate is postulated in the form as follows (cf. PERZYNA [49])

$$\dot{\epsilon}^p = \frac{1}{T} \langle \Phi \left[\frac{\tau}{\tau_Y(\epsilon^p, \vartheta, \beta, \xi)} - 1 \right] \rangle \mathrm{sgn}\tau, \tag{2.27}$$

where T is the relaxation time, $\langle\cdot\rangle$ denotes the Macauley bracket and τ_Y is the static yield-stress function. In this model the static yield-stress function depends on the inelastic strain $\in^p$, temperature ϑ, the density of obstacle dislocations β and the concentration of point defects ξ.

It is noteworthy that the empirical overstress function Φ can be determined basing on available experimental results performed under dynamic loading.

To describe the main experimentally observed facts connected with the macroscopic shear-band localization of single crystals, namely that the strain-hardening modulus rate h_{crit} at the inception of shear-band localization is positive and the direction of the localized shear-band is misaligned by some angle δ from the active slip system, we intend to consider the synergetic effects resulting from taking into account spatial covariance effects and thermomechanical couplings (cf. DUSZEK-PERZYNA and PERZYNA [14]).

To take into consideration the evolution of the substructure of crystals we introduce the density of mobile dislocations $\alpha^{(\nu)}$, the density of obstacle dislocations $\beta^{(\nu)}$ and the concentration of point defects $\xi^{(\nu)}$ for particular slip system ν as the internal state variables.

2.4. Heuristic considerations

From the analysis of the experimental investigations of localized shearing in single crystals performed by CHANG and ASARO [7, 8], SPITZIG [64], LISIECKI *et al.* [35] and RASHID *et al.* [57] we can follow the events in the order in which things naturally happen within a gauge length of the specimen during the uniaxial test, cf. Fig. 10.

In the first stage of the adiabatic inelastic flow process, a crystal specimen (a system) undergoes uniform extension and slip takes place. When control parameters are changed over a wide range, our system may run through a hierarchy of instabilities and accompanying cooperative phenomena. When we look at a microscopic level we observe that a crystal is well ordered, and is self-organized in microscopic shear-band pattern.

At the point when the load-engineering strain trajectory reaches its maximum, i.e. when the criterion of the onset of the localization by necking mode is satisfied, a crystal specimen exhibits slight amount of very diffuse symmetric necking.

With continued extension, the instability of inelastic flow process takes place and we observe on a macroscopic level the formation of adiabatic shear-band pattern within the diffusely necked region. A system is self-organized to a new two-phase material system (cf. Fig. 10). This is mainly due to different substructure and its evolution within the regions of adiabatic shear-bands when compared

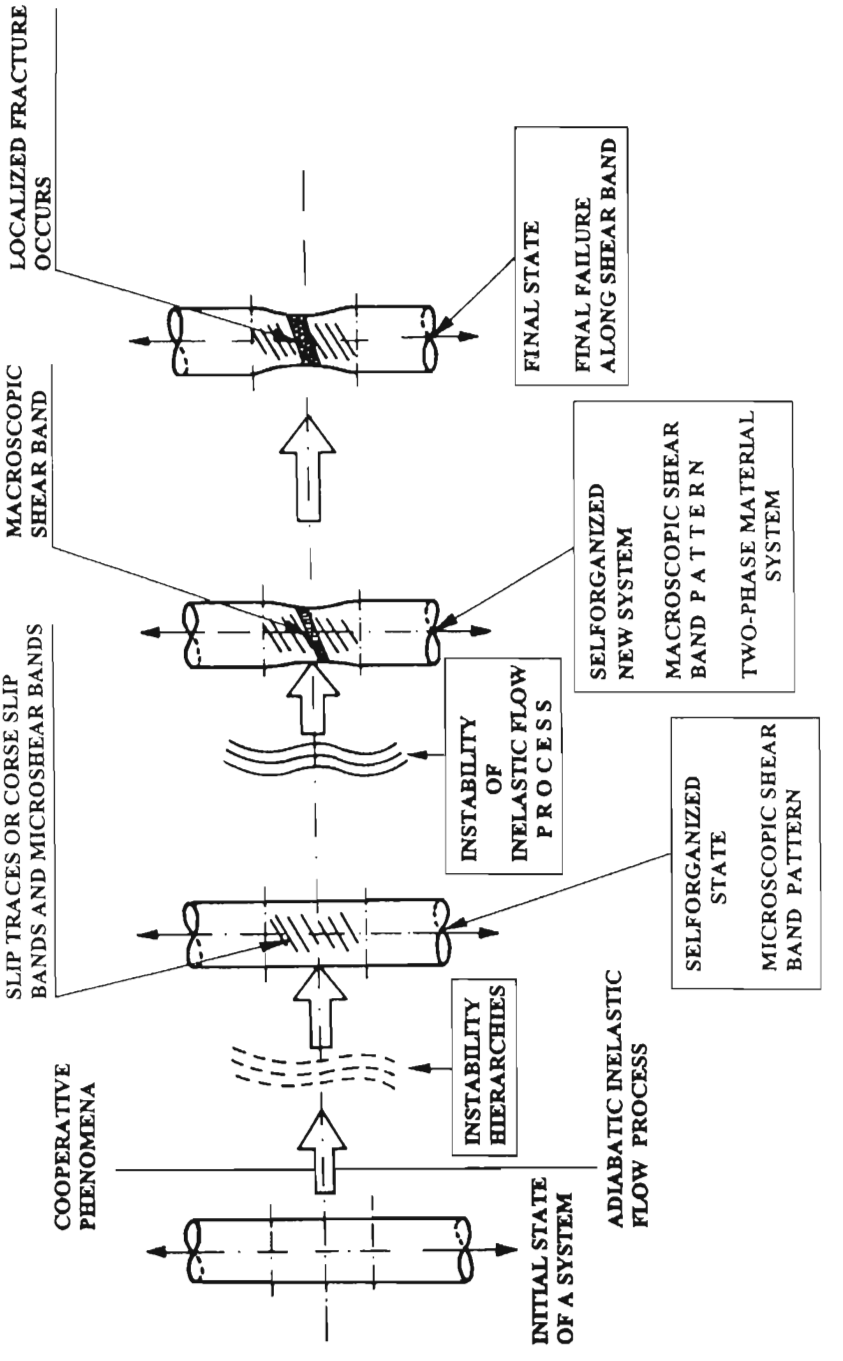

FIG. 10. Subsequent states of adiabatic inelastic flow process of single crystal.

with the substructure in the attached zones, cf. Fig. 8c. Final separation occurs by a ductile failure mechanism along the shear-band, cf. Figs. 4 and 5.

3. Kinematics of finite deformations and fundamental definitions

3.1. Fundamental measures of total deformation

Our notation will be as follows: $\mathcal{B}$ and $\mathcal{S}$ are manifolds, points in $\mathcal{B}$ are denoted by $\mathbf{X}$ and those in $\mathcal{S}$ by $\mathbf{x}$. The tangent spaces are written $T_{\mathbf{X}}\mathcal{B}$ and $T_{\mathbf{x}}\mathcal{S}$. Coordinate systems are denoted $\{X^A\}$ and $\{x^a\}$ for $\mathcal{B}$ and $\mathcal{S}$, respectively, with corresponding bases $\mathbf{E}_A$ and $\mathbf{e}_a$ and dual bases $\mathbf{E}^A$ and $\mathbf{e}^a$.

Let us take the Riemannian spaces on manifolds $\mathcal{B}$ and $\mathcal{S}$, i.e. $\{\mathcal{B}, \mathbf{G}\}$ and $\{\mathcal{S}, \mathbf{g}\}$, the metric tensors $\mathbf{G}$ and $\mathbf{g}$ are defined as follows $\mathbf{G} : T\mathcal{B} \to T^*\mathcal{B}$ and $\mathbf{g} : T\mathcal{S} \to T^*\mathcal{S}$, where $T\mathcal{B}$ and $T\mathcal{S}$ denote the tangent bundles of $\mathcal{B}$ and $\mathcal{S}$, respectively, and $T^*\mathcal{B}$ and $T^*\mathcal{S}$ their dual tangent bundles.

Let the metric tensor G_{AB} be defined by $G_{AB}(\mathbf{X}) = (\mathbf{E}_A, \mathbf{E}_B)_{\mathbf{X}}$, and similarly define g_{ab} by $g_{ab}(\mathbf{x}) = (\mathbf{e}_a, \mathbf{e}_b)_{\mathbf{x}}$, where $(\ ,\ )_{\mathbf{X}}$ and $(\ ,\ )_{\mathbf{x}}$ denote the standard inner products in $\mathcal{B}$ and $\mathcal{S}$, respectively.

Let

$$\mathbf{x} = \phi(\mathbf{X}, t) \tag{3.1}$$

be a regular motion, then $\phi_t : \mathcal{B} \to \mathcal{S}$ is a C^1 actual configuration (at time t) of $\mathcal{B}$ in $\mathcal{S}$. The tangent of ϕ is denoted by $\mathbf{F}$ and is called the deformation gradient of ϕ; thus $\mathbf{F} = T\phi$. For $\mathbf{X} \in \mathcal{B}$, we let $\mathbf{F}(\mathbf{X})$ denote the restriction of $\mathbf{F}$ to $T_{\mathbf{X}}\mathcal{B}$.

Thus

$$\mathbf{F}(\mathbf{X}, t) : T_{\mathbf{X}}\mathcal{B} \to T_{\mathbf{x}=\phi(\mathbf{X},t)}\mathcal{S} \tag{3.2}$$

is a linear transformation for each $\mathbf{X} \in \mathcal{B}$ and $t \in I \subset \mathbb{R}$. For each $\mathbf{X} \in \mathcal{B}$ there exists an orthogonal transformation $\mathbf{R}(\mathbf{X}) : T_{\mathbf{X}}\mathcal{B} \to T_{\mathbf{x}}\mathcal{S}$ such that $\mathbf{F} = \mathbf{R} \cdot \mathbf{U} = \mathbf{V} \cdot \mathbf{R}$. Notice that $\mathbf{U}$ and $\mathbf{V}$ operate within each fixed tangent space. We call $\mathbf{U}$ and $\mathbf{V}$ the right and left stretch tensor, respectively. For each $\mathbf{X} \in \mathcal{B}$, $\mathbf{U}(\mathbf{X}) : T_{\mathbf{X}}\mathcal{B} \to T_{\mathbf{X}}\mathcal{B}$ and for each $\mathbf{x} \in \mathcal{S}$, $\mathbf{V}(\mathbf{x}) : T_{\mathbf{x}}\mathcal{S} \to T_{\mathbf{x}}\mathcal{S}$.

The material (or Lagrangian) strain tensor $\mathbf{E} : T_{\mathbf{X}}\mathcal{B} \to T_{\mathbf{X}}\mathcal{B}$ is defined by

$$2\mathbf{E} = \mathbf{C} - \mathbf{I}, \quad (\mathbf{I} \text{ denotes the identity on } T_{\mathbf{X}}\mathcal{B}), \tag{3.3}$$

where

$$\mathbf{C} = \mathbf{F}^T \cdot \mathbf{F} = \mathbf{U}^2 = \mathbf{B}^{-1}. \tag{3.4}$$

The spatial (or Eulerian) strain tensor $\mathbf{e} : T_{\mathbf{x}}\mathcal{S} \to T_{\mathbf{x}}\mathcal{S}$ is defined by

$$2\mathbf{e} = \mathbf{i} - \mathbf{c}, \quad (\mathbf{i} \text{ denotes the identity on } T_{\mathbf{x}}\mathcal{S}), \tag{3.5}$$

where

$$\mathbf{c} = \mathbf{b}^{-1} \quad \text{and} \quad \mathbf{b} = \mathbf{F} \cdot \mathbf{F}^T = \mathbf{V}^2. \tag{3.6}$$

The various strain tensors can be redefined in terms of the pull-back and push-forward operations. For the material strain tensor $\mathbf{E}$ and the spatial strain tensor $\mathbf{e}$ we have

$$\begin{aligned} \mathbf{E}^\flat &= \phi^*(\mathbf{e}^\flat), & E_{AB}(\mathbf{X}) &= e_{ab}(\mathbf{x})F^a_A(\mathbf{X})F^b_B(\mathbf{X}), \\ \mathbf{e}^\flat &= \phi_*(\mathbf{E}^\flat), & e_{ab}(\mathbf{x}) &= E_{AB}(\mathbf{X})(\mathbf{F}(\mathbf{X})^{-1})^A_a(\mathbf{F}(\mathbf{X})^{-1})^B_b, \end{aligned} \tag{3.7}$$

where the symbol $\flat$ denotes the index lowering operator.

3.2. Finite elasto-viscoplastic deformation

Motivated by the micromechanics of single crystal plasticity we postulate a local multiplicative decomposition of the form

$$\mathbf{F}(\mathbf{X}, t) = \mathbf{F}^e(\mathbf{X}, t) \cdot \mathbf{F}^p(\mathbf{X}, t), \tag{3.8}$$

where $\mathbf{F}^{e-1}$ is interpreted as the local deformation that releases the stresses from each neighborhood $\mathcal{N}(\mathbf{x}) \subset \phi(\mathcal{B})$ in the current configuration of the body.

Let us consider a particle X, which at time $t = 0$ occupied the place $\mathbf{X}$ in the reference (material) configuration $\mathcal{B}$, its current place at time t in the actual (spatial) configuration $\mathcal{S}$ is $\mathbf{x} = \phi(\mathbf{X}, t)$, and its position in the unloaded actual configuration $\mathcal{S}'$ is denoted by $\mathbf{y}$. Thus we have

$$\mathbf{F}^e : T_{\mathbf{y}}\mathcal{S}' \to T_{\mathbf{x}}\mathcal{S}, \quad \mathbf{F}^p : T_{\mathbf{X}}\mathcal{B} \to T_{\mathbf{y}}\mathcal{S}', \tag{3.9}$$

where $T_{\mathbf{y}}\mathcal{S}'$ denotes the tangent space in the unloaded actual configuration $\mathcal{S}'$, cf. Fig. 11. It is noteworthy that $\mathbf{F}^e$ and $\mathbf{F}^p$ defined by (3.9) are linear transformations.

We shall treat the tangent space $T_{\mathbf{y}}\mathcal{S}'$ as an auxiliary tool which helps to define the plastic strain tensors[1)].

The plastic strain tensor $\mathbf{E}^p : T_{\mathbf{X}}\mathcal{B} \to T_{\mathbf{X}}\mathcal{B}$ is defined by

$$\mathbf{E}^p = \frac{1}{2}(\mathbf{C}^p - \mathbf{I}), \tag{3.10}$$

where

$$\mathbf{C}^p = \mathbf{F}^{p^T} \cdot \mathbf{F}^p = \mathbf{U}^{p^2} = \mathbf{B}^{p^{-1}} \quad \text{and} \quad \mathbf{E}^e \stackrel{\text{def}}{=} \mathbf{E} - \mathbf{E}^p. \tag{3.11}$$

[1)] For precise definition of the finite elasto-plastic deformation see PERZYNA [50]. Different approach to define the finite elasto-plastic deformation has been presented by Nemat-Nasser [43].

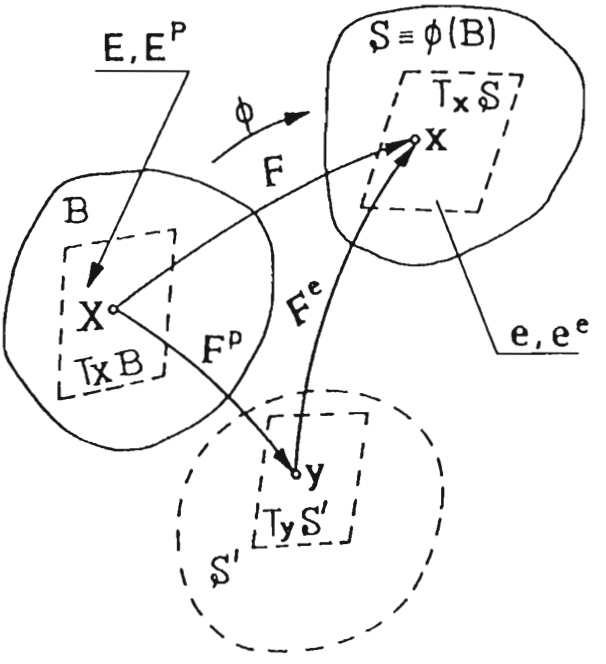

FIG. 11. Schematic representation of the multiplicative decomposition of the deformation gradient.

Similarly the elastic strain tensor $\mathbf{e}^e : T_x\mathcal{S} \to T_x\mathcal{S}$ is defined by

$$\mathbf{e}^e = \frac{1}{2}(\mathbf{i} - \mathbf{c}^e), \tag{3.12}$$

where

$$\mathbf{c}^e = \mathbf{b}^{e^{-1}}, \quad \mathbf{b}^e = \mathbf{F}^e \cdot \mathbf{F}^{e^T} = \mathbf{V}^{e^2} \quad \text{and} \quad \mathbf{e}^p \overset{\text{def}}{=} \mathbf{e} - \mathbf{e}^e. \tag{3.13}$$

The plastic tensors $\mathbf{E}^p$and $\mathbf{e}^p$ operate within each fixed tangent space; that is $\mathbf{E}^p : T_{\mathbf{X}}\mathcal{B} \to T_{\mathbf{X}}\mathcal{B}$ and $\mathbf{e}^p : T_{\mathbf{x}}\mathcal{S} \to T_{\mathbf{x}}\mathcal{S}$, cf. Fig. 11.

We can show that the following relations are valid

$$\phi_*(\mathbf{E}^{p^\flat}) = \mathbf{e}^{p^\flat}, \qquad \phi^*(\mathbf{e}^{e^\flat}) = \mathbf{E}^{e^\flat}. \tag{3.14}$$

3.3. Rates of the deformation tensor

Let $\phi(\mathbf{X}, t)$ be a C^2 motion of $\mathcal{B}$. Then the spatial velocity is $\boldsymbol{v}_t = \mathbf{V}_t \circ \phi_t^{-1}$, where $\mathbf{V}_t = \dfrac{\partial \phi}{\partial t}$ is the material velocity, i.e. $\boldsymbol{v} : \mathcal{S} \times I \to T\mathcal{S}$, $I \subset \mathbb{R}$.

The collection of maps $\phi_{t,s}$ such that for each s and $\mathbf{x}$, $t \to \phi_{t,s}(\mathbf{x})$ is an integral curve of $\boldsymbol{v}$, and $\phi_{s,s}(\mathbf{x}) = \mathbf{x}$, is called the flow or evolution operator of $\boldsymbol{v}$, i.e.

$$\{\phi_{t,s} \mid \phi_{t,s} = \phi_t \circ \phi_s^{-1} : \phi_s(\mathcal{B}) \to \phi_t(\mathcal{B})\} \tag{3.15}$$

and

$$\phi_{t,s} \circ \phi_{s,r} = \phi_{t,r}, \qquad \phi_{t,t} = \text{identity} \tag{3.16}$$

for all $r, s, t \in I \subset \mathbb{R}$.

If $\mathbf{t}$ is a C^1 (possibly time-dependent) tensor field on $\mathcal{S}$, then the Lie derivative of $\mathbf{t}$ with respect to $\boldsymbol{v}$ is defined by[2)]

$$\mathrm{L}_{\boldsymbol{v}}\mathbf{t} = \left(\frac{d}{dt}\phi_{t,s}^{*}\mathbf{t}_t\right)|_{t=s}\,. \tag{3.17}$$

If we hold t fixed in $\mathbf{t}_t$, we obtain the autonomous Lie derivative

$$\mathcal{L}_{\boldsymbol{v}}\mathbf{t} = \left(\frac{d}{dt}\phi_{t,s}^{*}\mathbf{t}_s\right)|_{t=s}\,. \tag{3.18}$$

Thus

$$\mathrm{L}_{\boldsymbol{v}}\mathbf{t} = \frac{\partial \mathbf{t}}{\partial t} + \mathcal{L}_{\boldsymbol{v}}\mathbf{t}. \tag{3.19}$$

If $\mathbf{t} \in \mathbf{T}^r{}_s(\mathcal{S})$ (elements of $\mathbf{T}^r{}_s(\mathcal{S})$ are called tensors on $\mathcal{S}$, contravariant of order r and covariant of order s) then $\mathrm{L}_{\boldsymbol{v}}\mathbf{t} \in \mathbf{T}^r{}_s(\mathcal{S})$.

The spatial velocity gradient $\mathbf{l}$ is defined by

$$\mathbf{l} = D\boldsymbol{v} : T_{\mathbf{x}}\mathcal{S} \to T_{\mathbf{x}}\mathcal{S}, \quad \text{i.e.} \quad l^a_b = v^a\,|_b = \frac{\partial v^a}{\partial x^b} + \gamma^a_{bc}v^c, \tag{3.20}$$

where γ^a_{bc} denotes the Christoffel symbol for $\mathbf{g}$.

The spatial velocity gradient $\mathbf{l}$ can be expressed as follows

$$\begin{aligned}\mathbf{l} = D\boldsymbol{v} = \dot{\mathbf{F}} \cdot \mathbf{F}^{-1} = \dot{\mathbf{F}}^e \cdot \mathbf{F}^{e^{-1}} + \mathbf{F}^e \cdot (\dot{\mathbf{F}}^p \cdot \mathbf{F}^{p^{-1}}) \cdot \mathbf{F}^{e^{-1}} = \mathbf{l}^e + \mathbf{l}^p \\ = \mathbf{d} + \boldsymbol{\omega} = \mathbf{d}^e + \boldsymbol{\omega}^e + \mathbf{d}^p + \boldsymbol{\omega}^p,\end{aligned} \tag{3.21}$$

where $\mathbf{d}$ denotes the spatial rate of deformation tensor and $\boldsymbol{\omega}$ is called the spin.

[2)] The algebraic and dynamic interpretations of the Lie derivative have been presented by Abraham *et al.* [1], cf. also MARSDEN and HUGHES [36].

Let us define the material (or Lagrangian) rate of deformation tensor $\mathbf{D}$ as follows

$$\mathbf{D}(\mathbf{X},t) = \frac{\partial}{\partial t}\mathbf{E}(\mathbf{X},t). \tag{3.22}$$

We have a very important relation

$$\mathbf{d}^\flat = \mathrm{L}_{\boldsymbol{\upsilon}}\mathbf{e}^\flat = \phi_*\frac{\partial}{\partial t}(\phi^*\mathbf{e}^\flat) = \phi_*(\frac{\partial}{\partial t}\mathbf{E}^\flat) = \phi_*(\mathbf{D}^\flat). \tag{3.23}$$

On the other hand

$$\mathbf{d}^\flat = \mathrm{L}_{\boldsymbol{\upsilon}}\mathbf{e}^\flat = \mathrm{L}_{\boldsymbol{\upsilon}}\left[\frac{1}{2}\left(\mathbf{g}-\mathbf{b}^{-1}\right)\right]^\flat = \frac{1}{2}\mathrm{L}_{\boldsymbol{\upsilon}}\mathbf{g} = \frac{1}{2}\left(g_{cb}\upsilon^c\,|_a + g_{ac}\upsilon^c\,|_b\right)\mathbf{e}^a\otimes\mathbf{e}^b, \tag{3.24}$$

i.e. the symmetric part of the velocity gradient $\mathbf{l}$.

The components of the spin $\boldsymbol{\omega}$ are given by

$$\omega_{ab} = \frac{1}{2}\left(g_{ac}\upsilon^c\,|_b - g_{cb}\upsilon^c\,|_a\right) = \frac{1}{2}\left(\frac{\partial\upsilon_a}{\partial x^b} - \frac{\partial\upsilon_b}{\partial x^a}\right), \tag{3.25}$$

and

$$\mathbf{d}^{e^\flat} = \mathrm{L}_{\boldsymbol{\upsilon}}\mathbf{e}^{e^\flat}, \qquad \mathbf{d}^{p^\flat} = \mathrm{L}_{\boldsymbol{\upsilon}}\mathbf{e}^{p^\flat}. \tag{3.26}$$

3.4. Application to single crystal behaviour

A fundamental principle of the description of the thermomechanical, elasto-plastic behaviour of crystals had been introduced by Taylor [65]. He postulated that material flows through the crystal lattice via the dislocation motion, whereas the lattice itself, with the material embedded in it, undergoes elastic deformations and rotations. Thus there are two physically different mechanisms for deforming and reorienting the material of a crystal, namely plastic slip and lattice deformation. Of course, single crystals can be generally subjected to rigid body rotations owing to the boundary constraints or compatibility requirements. Then, it may be convenient (although arbitrary) to consider this as the third mechanism (cf. ASARO [2], PEIRCE *et al.* [46, 47]). In this presentation we have not taken the third mechanism into account.

It is noteworthy that a local multiplicative decomposition of the form (3.8) is just motivated by the micromechanics of single crystal plasticity. It is understood that $\mathbf{F}^e$ is the lattice contribution to $\mathbf{F}$, and is associated with stretching and

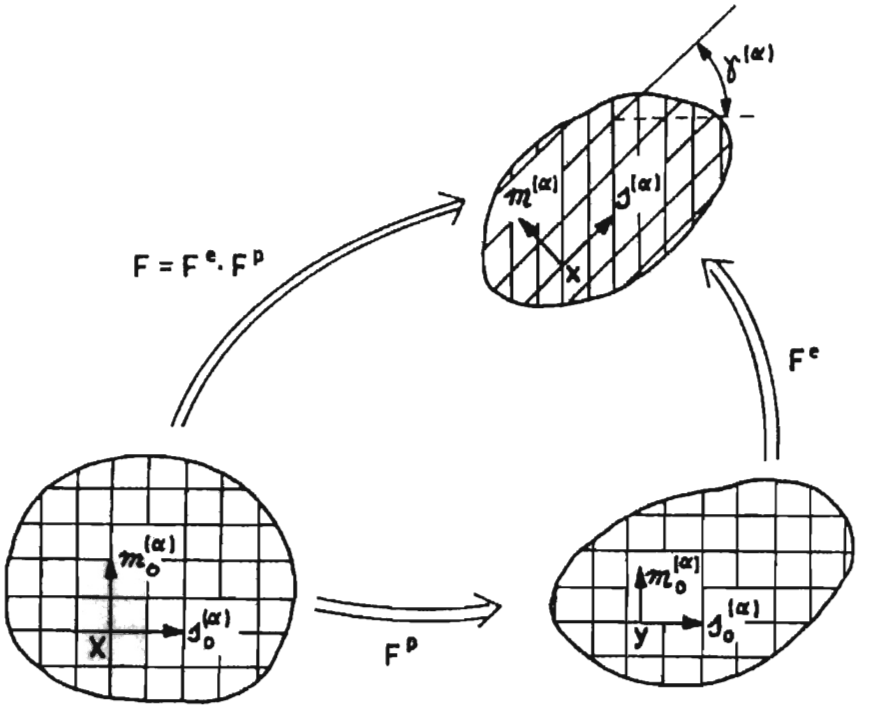

FIG. 12. Decomposition of the deformation gradient for single crystal.

rotation of the crystal lattice, $\mathbf{F}^p$ describes the deformation solely due to plastic shearing on crystallographic slip systems, cf. Fig. 12.

A particular slip system α is specified by the slip vectors $\mathbf{s}_0^{(\alpha)}$, $\mathbf{m}_0^{(\alpha)}$, where $\mathbf{s}_0^{(\alpha)}$ gives the slip direction and $\mathbf{m}_0^{(\alpha)}$ is the slip plane normal. Let $\mathbf{z}_0^{(\alpha)}$ be a unit vector perpendicular to $\mathbf{s}_0^{(\alpha)}$ and $\mathbf{m}_0^{(\alpha)}$ in Fig. 12 so that $\mathbf{s}_0^{(\alpha)}$, $\mathbf{m}_0^{(\alpha)}$, $\mathbf{z}_0^{(\alpha)}$ form a right-handed triad. Thus the vectors $\mathbf{s}_0^{(\alpha)}$, $\mathbf{m}_0^{(\alpha)}$ and $\mathbf{z}_0^{(\alpha)}$ in the undeformed lattice are taken to be orthonormal.

As the crystal deforms, the vectors $\mathbf{s}^{(\alpha)}$ and $\mathbf{m}^{(\alpha)}$ are stretched and rotated according to $\mathbf{F}^e$. In the deformed lattice we have

$$\mathbf{s}^{(\alpha)} = \mathbf{F}^e \cdot \mathbf{s}_0^{(\alpha)}, \qquad \mathbf{m}^{(\alpha)} = \mathbf{m}_0^{(\alpha)} \cdot (\mathbf{F}^e)^{-1}. \tag{3.27}$$

Using Eq. (3.21) we define the elastic part of the velocity gradient as follows

$$\mathbf{l}^e = \dot{\mathbf{F}}^e \cdot \mathbf{F}^{e-1} \tag{3.28}$$

and postulate for the plastic part

$$\mathbf{l}^p = \dot{\mathbf{F}} \cdot \mathbf{F}^{-1} - \dot{\mathbf{F}}^e \cdot \mathbf{F}^{e-1} = \mathbf{F}^e \cdot \dot{\mathbf{F}}^p \cdot \mathbf{F}^{p-1} \cdot \mathbf{F}^{e-1} = \sum_{\alpha=1}^{n} \mathbf{s}^{(\alpha)} \mathbf{m}^{(\alpha)} \dot{\gamma}^{(\alpha)}, \tag{3.29}$$

where $\dot{\gamma}^{(\alpha)}$ is the rate of shearing on the slip system α.

The elastic rates of stretching and spin $\mathbf{d}^e$ and $\boldsymbol{\omega}^e$ are the symmetric and anti-symmetric parts of $\dot{\mathbf{F}}^e \cdot \mathbf{F}^{e-1}$, respectively. The plastic parts of the rate of stretching and spin are determined by the relations

$$\mathbf{d}^p = \sum_{\alpha=1}^{n} \dot{\gamma}^{(\alpha)} \mathbf{N}^{(\alpha)}, \qquad \boldsymbol{\omega}^p = \sum_{\alpha=1}^{n} \dot{\gamma}^{(\alpha)} \mathbf{W}^{(\alpha)}, \tag{3.30}$$

where

$$\mathbf{N}^{\alpha} = \frac{1}{2}\left[\mathbf{s}^{(\alpha)}\mathbf{m}^{(\alpha)} + \mathbf{m}^{(\alpha)}\mathbf{s}^{(\alpha)}\right], \qquad \mathbf{W}^{\alpha} = \frac{1}{2}\left[\mathbf{s}^{(\alpha)}\mathbf{m}^{(\alpha)} - \mathbf{m}^{(\alpha)}\mathbf{s}^{(\alpha)}\right]. \tag{3.31}$$

Of course, the schematic decomposition of the deformation gradient for single crystal shown in Fig. 12 is directly related to the appropriate decomposition represented in Fig. 11. In the points $\mathbf{X}$, $\mathbf{x}$ and $\mathbf{y}$, i.e. in the reference, actual and unloaded configurations, respectively, of the considered body, in Fig. 12 the crystalline structure of the single crystal and its deformation is explicitly presented.

3.5. Stress tensors and the resolved Schmid stress

The first Piola-Kirchhoff stress tensor P^{aA} is the two-point tensor obtained by performing a Piola transformation on the second index of the Cauchy stress tensor $\boldsymbol{\sigma}$, i.e.

$$P^{aA} = J(\mathbf{F}^{-1})^A_b \sigma^{ab}, \tag{3.32}$$

where J denotes the Jacobian of the deformation.

The second Piola-Kirchhoff stress tensor $\mathbf{S}$ is defined as follows:

$$S^{AB} = (\mathbf{F}^{-1})^A_a P^{aB} = J(\mathbf{F}^{-1})^A_a (\mathbf{F}^{-1})^B_b \sigma^{ab} = (\mathbf{F}^{-1})^A_a (\mathbf{F}^{-1})^B_b \tau^{ab}, \tag{3.33}$$

i.e.

$$\mathbf{S} = \phi^*(\boldsymbol{\tau}), \tag{3.34}$$

where $\boldsymbol{\tau} = J\boldsymbol{\sigma}$ is called the Kirchhoff stress tensor.

Let us take the rate of stress working per unit reference volume

$$\boldsymbol{\tau} : \mathbf{d} = \boldsymbol{\tau} : \mathbf{d}^e + \boldsymbol{\tau} : \mathbf{d}^p = \boldsymbol{\tau} : \mathbf{d}^e + \sum_{\alpha=1}^{n} \tau^{(\alpha)} \dot{\gamma}^{(\alpha)}, \tag{3.35}$$

where

$$\tau^{(\alpha)} = \boldsymbol{\tau} : \mathbf{N}^{(\alpha)} \tag{3.36}$$

is the Schmid resolved stress on the slip system α.

3.6. Rates of stress tensors

The rate of the Kirchhoff stress tensor $\boldsymbol{\tau}$ is given by

$$\mathrm{L}_{\boldsymbol{v}}\boldsymbol{\tau} = \phi_* \frac{\partial}{\partial t}(\phi^* \boldsymbol{\tau}) = \phi_*(\frac{\partial}{\partial t}\mathbf{S}) = \mathbf{F} \cdot (\frac{\partial}{\partial t}\mathbf{S}) \cdot \mathbf{F}^T \circ \phi_t^{-1}. \tag{3.37}$$

Let us define

$$\begin{aligned} \boldsymbol{\tau}_1 &= \tau^{ab}\mathbf{e}_a \otimes \mathbf{e}_b \in \mathbf{T}^2{}_0(\mathcal{S}), \\ \boldsymbol{\tau}_2 &= \tau_a{}^b\mathbf{e}^a \otimes \mathbf{e}_b \in \mathbf{T}_1{}^1(\mathcal{S}), \\ \boldsymbol{\tau}_3 &= \tau^a{}_b\mathbf{e}_a \otimes \mathbf{e}^b \in \mathbf{T}^1{}_1(\mathcal{S}). \end{aligned} \tag{3.38}$$

Then

$$(\mathrm{L}_{\boldsymbol{v}}\boldsymbol{\tau}_1)^{ab} = \frac{\partial \tau^{ab}}{\partial t} + \frac{\partial \tau^{ab}}{\partial x^c}v^c - \tau^{cb}\frac{\partial v^a}{\partial x^c} - \tau^{ac}\frac{\partial v^b}{\partial x^c} \tag{3.39}$$

is the rate associated with the name of Oldroyd (cf. OLDROYD [45]). The Zaremba-Jaumann rate (cf. ZAREMBA [71, 72] and JAUMANN [32]) is defined as follows

$$\frac{1}{2}\left[(\mathrm{L}_{\boldsymbol{v}}\boldsymbol{\tau}_3)^a{}_c g^{cb} + g^{ac}(\mathrm{L}_{\boldsymbol{v}}\boldsymbol{\tau}_2)_c{}^b\right] = \frac{\partial \tau^{ab}}{\partial t} + \frac{\partial \tau^{ab}}{\partial x^c}v^c + \tau^{ad}\omega_d{}^b - \tau^{db}\omega^a{}_d. \tag{3.40}$$

4. CONSTITUTIVE STRUCTURE OF INELASTIC SINGLE CRYSTALS

4.1. Constitutive postulates

Let us assume that the laws of: (i) conservation of mass, (ii) balance of momentum, (iii) balance of moment of momentum, (iv) balance of energy, (v) entropy production inequality, hold true.

We introduce the four fundamental postulates:

(i) Existence of the free energy function. It is assumed that the free energy function is given by [3)]

$$\psi = \hat{\psi}(\mathbf{e}, \mathbf{F}, \vartheta; \gamma^{(\nu)}, \alpha^{(\nu)}, \beta^{(\nu)}, \xi^{(\nu)}), \tag{4.1}$$

where $\mathbf{e}$ denotes the Eulerian strain tensor, $\mathbf{F}$ is deformation gradient, ϑ temperature and $\gamma^{(\nu)}$ denotes the shearing on slip system ν, $\alpha^{(\nu)}$ is the density of mobile dislocations and $\beta^{(\nu)}$ the density of obstacle dislocations for particular slip system ν, and $\xi^{(\nu)}$ denotes the concentration of point defects for slip system ν.

[3)] For a similar idea see TEODOSIU and SIDOROFF [67].

(ii) Axiom of objectivity (spatial covariance). The constitutive structure should be invariant under any diffeomorphism (any motion) $\xi : \mathcal{S} \to \mathcal{S}$ (MARSDEN and HUGHES [36]), cf. Fig. 13. Assuming that $\xi : \mathcal{S} \to \mathcal{S}$ is a regular, orientation preserving map transforming $\mathbf{x}$ into $\mathbf{x}'$ and $T\xi$ is an isometry from $T_{\mathbf{x}}\mathcal{S}$ to $T_{\mathbf{x}'}\mathcal{S}$, we obtain the axiom of material frame indifference (cf. TRUESDELL and NOLL [69]).

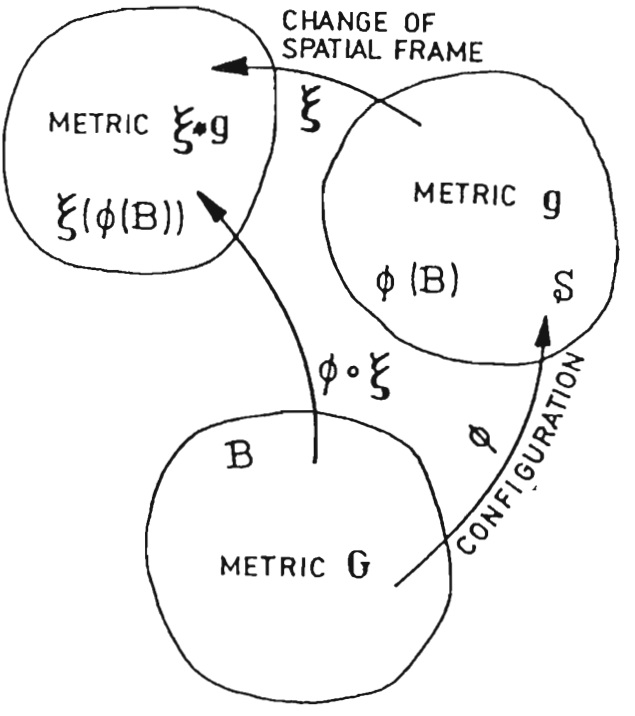

FIG. 13. Schematic representation of the change of spatial frame generated by superposed spatial diffeomerphism.

(iii) The axiom of the entropy production. For any regular motion of a single crystal (denoted by $\mathcal{B}$), the constitutive functions are assumed to satisfy the reduced dissipation inequality

$$\frac{1}{\rho_{\mathrm{Ref}}}\boldsymbol{\tau} : \mathbf{d} - (\eta\dot{\vartheta} + \dot{\psi}) - \frac{1}{\rho\vartheta}\mathbf{q} \cdot \mathrm{grad}\vartheta \geq 0, \tag{4.2}$$

where ρ_{Ref} and ρ denote the mass density in the reference and actual configuration, respectively, $\boldsymbol{\tau}$ is the Kirchhoff stress tensor, $\mathbf{d}$ the rate of deformation, η is the specific (per unit mass) entropy, and $\mathbf{q}$ denotes the

heat flow vector field. MARSDEN and HUGHES [36] proved that the reduced dissipation inequality (4.2) is equivalent to the entropy production inequality, first introduced by COLEMAN and NOLL [10] in the form of the Clausius-Duhem inequality. In fact the Clausius-Duhem inequality gives a statement of the second law of thermodynamics within the framework of mechanics of continuous media.

As it has been pointed out by MARSDEN and HUGHES [36], the question how one should set the basic principles of thermodynamics has given rise to much controversy (see e.g. MÜLLER [40] and GREEN and NAGHDI [23]). Alternative theories have been proposed e.g. by GREEN and NAGHDI [23, 24], MÜLLER [40, 41], SERRIN [62] and DAY and SILHAVY [12], cf. also an exhaustive discussion on the subject given by TRUESDELL [68].

(iv) The evolution equations for the internal state variables are assumed in the form as follows:[4)]

$$
\begin{aligned}
\dot{\alpha}^{(\nu)} &= \sum_{\delta=1}^{n} a_1^{(\nu\delta)}\dot{\gamma}^{(\delta)} + a_2^{(\nu)}\dot{\vartheta} + \sum_{\delta=1}^{n} a_3^{(\nu\delta)}\dot{\beta}^{(\delta)} + \sum_{\delta=1}^{n} a_4^{(\nu\delta)}\dot{\xi}^{(\delta)},\\
\dot{\beta}^{(\nu)} &= \sum_{\delta=1}^{n} b_1^{(\nu\delta)}\dot{\gamma}^{(\delta)} + b_2^{(\nu)}\dot{\vartheta} + \sum_{\delta=1}^{n} b_3^{(\nu\delta)}\dot{\alpha}^{(\delta)} + \sum_{\delta=1}^{n} b_4^{(\nu\delta)}\dot{\xi}^{(\delta)},\\
\dot{\xi}^{(\nu)} &= \sum_{\delta=1}^{n} c_1^{(\nu\delta)}\dot{\gamma}^{(\delta)} + c_2^{(\nu)}\dot{\vartheta} + \sum_{\delta=1}^{n} c_3^{(\nu\delta)}\dot{\alpha}^{(\delta)} + \sum_{\delta=1}^{n} c_4^{(\nu\delta)}\dot{\beta}^{(\delta)},\\
\dot{\gamma}^{(\nu)} &= \frac{1}{T^{(\nu)}}\langle\Phi\left[\frac{\tau^{(\nu)}}{\tau_c^{(\nu)}(\gamma,\beta,\xi,\vartheta) + \boldsymbol{\kappa}^{(\nu)} : \boldsymbol{\tau}} - 1\right]\rangle \operatorname{sgn}\tau^{(\nu)},
\end{aligned}
\tag{4.3}
$$

where $\gamma = \sum_{\nu=1}^{n}\gamma^{(\nu)}$, $\beta = \sum_{\nu=1}^{n}\beta^{(\nu)}$, $\xi = \sum_{\nu=1}^{n}\xi^{(\nu)}$, $\tau^{(\nu)}$ denotes the Schmid resolved shear stress on the slip system ν, $\tau_c^{(\nu)}$ is the yield-stress function on the slip system ν, $\boldsymbol{\kappa}^{(\nu)}$ is the symmetric tensor of non-Schmid effects and the coefficients a_i, b_i, c_i $(i = 1, 2, 3, 4)$ are material functions.

4.2. Rate-type constitutive relations

Suppose the axiom of the entropy production holds. Then the constitutive assumption (4.1) and the evolution equations (4.4) lead to the results as follows:

[4)] Particular case of the evolution equations for densities of dislocations $(4.4)_{1,2}$ has been considered by ESTRIN and KUBIN [17] and BALKE and ESTRIN [4].

$$\boldsymbol{\tau} = \rho_{Ref}\frac{\partial\hat{\psi}}{\partial\mathbf{e}}, \qquad \eta = -\frac{\partial\hat{\psi}}{\partial\vartheta},$$
$$\vartheta\hat{i} - \frac{1}{\rho\vartheta}\mathbf{q}\cdot\operatorname{grad}\vartheta \geq 0, \tag{4.4}$$

where

$$\vartheta\hat{i} = -\sum_{\nu=1}^{n}\frac{\partial\hat{\psi}}{\partial\gamma^{(\nu)}}\dot{\gamma}^{(\nu)} - \sum_{\nu=1}^{n}\frac{\partial\hat{\psi}}{\partial\alpha^{(\nu)}}\dot{\alpha}^{(\nu)} - \sum_{\nu=1}^{n}\frac{\partial\hat{\psi}}{\partial\beta^{(\nu)}}\dot{\beta}^{(\nu)} - \sum_{\nu=1}^{n}\frac{\partial\hat{\psi}}{\partial\xi^{(\nu)}}\dot{\xi}^{(\nu)} \tag{4.5}$$

denotes the rate of internal dissipation.

We take here advantage of the thermodynamic restrictions on materials described by internal state variables presented by COLEMAN and GURTIN [9].

Operating with the Lie derivative on the stress relation $(4.5)_1$ and keeping the internal state variables constant, we obtain[5] (cf. DUSZEK-PERZYNA and PERZYNA [14])

$$\mathrm{L}_{\mathcal{U}}\boldsymbol{\tau} = \mathcal{L}^{e} : \mathbf{d} - \mathcal{L}^{th}\dot{\vartheta} - \sum_{\beta=1}^{n}\left[\mathcal{L}^{e} : \mathbf{N}^{(\beta)} + \mathbf{b}^{(\beta)}\right]\dot{\gamma}^{(\beta)}, \tag{4.6}$$

where

$$\mathcal{L}^{e} = \rho_{Ref}\frac{\partial^{2}\hat{\psi}}{\partial\mathbf{e}^{2}}, \qquad \mathcal{L}^{th} = -\rho_{Ref}\frac{\partial^{2}\hat{\psi}}{\partial\mathbf{e}\partial\vartheta},$$
$$\mathbf{b}^{(\beta)} = (\mathbf{N}^{(\beta)} + \mathbf{W}^{(\beta)})\cdot\boldsymbol{\tau} + \boldsymbol{\tau}\cdot(\mathbf{N}^{(\beta)} - \mathbf{W}^{(\beta)}). \tag{4.7}$$

Operating on the entropy relation $(4.5)_2$ with the Lie derivative and substituting the result into the energy balance equation, we obtain

$$\begin{aligned}\rho c_{p}\dot{\vartheta} = -\operatorname{div}\mathbf{q} + \vartheta\frac{\rho}{\rho_{Ref}}\frac{\partial\boldsymbol{\tau}}{\partial\vartheta} : \mathbf{d} + \chi\sum_{\nu=1}^{n}\tau^{(\nu)}\dot{\gamma}^{(\nu)} \\ + \chi^{*}\sum_{\nu=1}^{n}\sum_{\delta=1}^{n}(a_{1}^{-1})^{(\nu\delta)}\tau^{(\delta)}\dot{\alpha}^{(\nu)} + \chi^{**}\sum_{\nu=1}^{n}\sum_{\delta=1}^{n}(b_{1}^{-1})^{(\nu\delta)}\tau^{(\delta)}\dot{\beta}^{(\nu)} \\ + \chi^{***}\sum_{\nu=1}^{n}\sum_{\delta=1}^{n}(c_{1}^{-1})^{(\nu\delta)}\tau^{(\delta)}\dot{\xi}^{(\nu)},\end{aligned} \tag{4.8}$$

[5] Particular case of the rate equation (4.6) has been presented by Hill and RICE [31].

where

$$
\begin{aligned}
c_p &= -\vartheta \frac{\partial^2 \hat{\psi}}{\partial \vartheta^2}, \qquad \chi\tau^{(\nu)} = -\rho \left(\frac{\partial \hat{\psi}}{\partial \gamma^{(\nu)}} - \vartheta \frac{\partial^2 \hat{\psi}}{\partial \vartheta \partial \gamma^{(\nu)}} \right), \\
\chi^* \tau^{(\nu)} &= -\rho \sum_{\delta=1}^{n} a_1^{(\nu\delta)} \left(\frac{\partial \hat{\psi}}{\partial \alpha^{(\delta)}} - \vartheta \frac{\partial^2 \hat{\psi}}{\partial \vartheta \partial \alpha^{(\delta)}} \right), \\
\chi^{**} \tau^{(\nu)} &= -\rho \sum_{\delta=1}^{n} b_1^{(\nu\delta)} \left(\frac{\partial \hat{\psi}}{\partial \beta^{(\delta)}} - \vartheta \frac{\partial^2 \hat{\psi}}{\partial \vartheta \partial \beta^{(\delta)}} \right), \\
\chi^{***} \tau^{(\nu)} &= -\rho \sum_{\delta=1}^{n} c_1^{(\nu\delta)} \left(\frac{\partial \hat{\psi}}{\partial \xi^{(\delta)}} - \vartheta \frac{\partial^2 \hat{\psi}}{\partial \vartheta \partial \xi^{(\delta)}} \right).
\end{aligned} \tag{4.9}
$$

A set of equations (4.4), (4.6) and (4.8) generalizes the "Duhamel-Neumann hypothesi" for inelastic single crystals, cf. SOKOLNIKOFF [63], p.359 and MARSDEN and HUGHES [36], p.204. It is noteworthy that this generalization takes account of the effects as follows: (i) thermomechanical couplings; (ii) evolution of the dislocation substructure; (iii) influence of covariance terms, lattice deformation and rotation, and plastic spin; (iv) deviation from the Schmid rule of a critical resolved shear stress for slip; and (v) rate sensitivity (viscosity).

4.3. Analysis of thermomechanical couplings

To show synergetic effects generated by cooperative phenomena of thermomechanical couplings and the influence of the evolution of the dislocation substructure, let us consider the evolution equations for the internal state variables $\alpha^{(\nu)}$, $\beta^{(\nu)}$ and $\xi^{(\nu)}$, cf. Eqs. $(4.4)_{1-3}$. These equations can be written in the form as follows:

$$
\begin{aligned}
\dot{\alpha}^{(\nu)} &= \sum_{\delta=1}^{n} A_1^{(\nu\delta)} \dot{\gamma}^{(\delta)} + A_2^{(\nu)} \dot{\vartheta}, \\
\dot{\beta}^{(\nu)} &= \sum_{\delta=1}^{n} B_1^{(\nu\delta)} \dot{\gamma}^{(\delta)} + B_2^{(\nu)} \dot{\vartheta}, \\
\dot{\xi}^{(\nu)} &= \sum_{\delta=1}^{n} C_1^{(\nu\delta)} \dot{\gamma}^{(\delta)} + C_2^{(\nu)} \dot{\vartheta},
\end{aligned} \tag{4.10}
$$

where

$$
\begin{aligned}
\mathbf{A}_1 &= \overline{\mathbf{A}}^{-1} \cdot \mathrm{A}_3^{-1} \left(\mathrm{A}_1 + \mathrm{A}_4 \cdot \mathrm{B}_4^{-1} \cdot \mathrm{B}_1\right), \\
\mathbf{A}_2 &= \overline{\mathbf{A}}^{-1} \cdot \mathrm{A}_3^{-1} \left(\mathrm{A}_2 + \mathrm{A}_4 \cdot \mathrm{B}_4^{-1} \cdot \mathrm{B}_2\right), \\
\mathbf{B}_1 &= \overline{\mathbf{B}}^{-1} \cdot \mathrm{B}_4^{-1} \left(\mathrm{B}_1 + \mathrm{B}_3 \cdot \mathrm{A}_3^{-1} \cdot \mathrm{A}_1\right), \\
\mathbf{B}_2 &= \overline{\mathbf{B}}^{-1} \cdot \mathrm{B}_4^{-1} \left(\mathrm{B}_2 + \mathrm{B}_3 \cdot \mathrm{A}_3^{-1} \cdot \mathrm{A}_2\right), \\
\mathbf{C}_1 &= \mathbf{c}_1 + \mathbf{c}_3 \cdot \mathbf{A}_1 + c_4 \cdot \mathbf{B}_1, \\
\mathbf{C}_2 &= \mathbf{c}_2 + \mathbf{c}_3 \cdot \mathbf{A}_2 + c_4 \cdot \mathbf{B}_2,
\end{aligned}
\tag{4.11}
$$

and

$$
\begin{aligned}
&\mathrm{A}_1 = \mathbf{a}_1 + \mathbf{a}_4 \cdot \mathbf{c}_1, \qquad \mathrm{A}_2 = \mathbf{a}_2 + \mathbf{a}_4 \cdot \mathbf{c}_2, \\
&\mathrm{B}_1 = \mathbf{b}_1 + \mathbf{b}_4 \cdot \mathbf{c}_1, \qquad \mathrm{B}_2 = \mathbf{b}_2 + \mathbf{b}_4 \cdot \mathbf{c}_2, \\
&\mathrm{A}_3 = \mathbf{1} - \mathbf{a}_4 \cdot \mathbf{c}_3, \qquad \mathrm{A}_4 = \mathbf{a}_3 + \mathbf{a}_4 \cdot \mathbf{c}_4, \\
&\mathrm{B}_3 = \mathbf{b}_3 + \mathbf{b}_4 \cdot \mathbf{c}_3, \qquad \mathrm{B}_4 = \mathbf{1} - \mathbf{b}_4 \cdot \mathbf{c}_4,
\end{aligned}
\tag{4.12}
$$

$$
\overline{\mathbf{A}} = \mathbf{1} - \mathrm{A}_3^{-1} \cdot \mathrm{A}_4 \cdot \mathrm{B}_4^{-1} \cdot \mathrm{B}_3, \qquad \overline{\mathbf{B}} = \mathbf{1} - \mathrm{B}_4^{-1} \cdot \mathrm{B}_3 \cdot \mathrm{A}_3^{-1} \cdot \mathrm{A}_4.
$$

Substituting (4.10) into (4.8) gives the fundamental rate equation for temperature ϑ in the form

$$
(\rho c_p - \lambda)\dot{\vartheta} = -\mathrm{div}\mathbf{q} + \vartheta \frac{\rho}{\rho_{Ref}} \frac{\partial \boldsymbol{\tau}}{\partial \vartheta} : \mathbf{d} + \chi \boldsymbol{\tau} : \mathbf{d}^p + \sum_{\nu=1}^{n} \sum_{\kappa=1}^{n} \Lambda^{(\delta\kappa)} \tau^{(\delta)} \dot{\gamma}^{(\kappa)}
\tag{4.13}
$$

with the denotations as follows:

$$
\begin{aligned}
\lambda = \sum_{\nu=1}^{n} \sum_{\delta=1}^{n} \Big[& \chi^{*} \left(a_1^{-1}\right)^{(\nu\delta)} A_2^{(\nu)} \\
& + \chi^{**} \left(b_1^{-1}\right)^{(\nu\delta)} B_2^{(\nu)} + \chi^{***} \left(c_1^{-1}\right)^{(\nu\delta)} C_2^{(\nu)} \Big] \tau^{(\delta)},
\end{aligned}
\tag{4.14}
$$

$$
\begin{aligned}
\Lambda^{(\delta\kappa)} = \sum_{\nu=1}^{n} \Big[& \chi^{*} \left(a_1^{-1}\right)^{(\nu\delta)} A_1^{(\nu\kappa)} \\
& + \chi^{**} \left(b_1^{-1}\right)^{(\nu\delta)} B_1^{(\nu\kappa)} + \chi^{***} \left(c_1^{-1}\right)^{(\nu\delta)} C_1^{(\nu\kappa)} \Big].
\end{aligned}
$$

Let us interpret each term of Eq. (4.13). On the left-hand side of Eq. (4.13) we have the term $(\rho c_p - \lambda)\dot{\vartheta}$ which represents the heat rate conversion minus the internal heating lost for the generation of new dislocations and point defects. The first term on the right-hand side represents the heat conduction effects induced

by the heat flux vector $\mathbf{q}$. The second term on the right-hand side of Eq. (4.13) is caused by the dependence of the stress tensor $\boldsymbol{\tau}$ on temperature and is not of a dissipative nature. The third term on the right-hand side represents the rate of internal dissipation due to plastic flow process, while the last term gives the contribution to the rate of internal dissipation generated by the evolution of the dislocation substructure.

This interpretation can be more understandable when we look at the character of the coefficients λ and $\Lambda^{(\delta k)}$. Both of them account for the evolution of the dislocation substructure, the first due to the transient thermal effects, the second being attributed to the influence of plastic flow phenomena.

5. Rate-independent response of single crystals

The viscoplastic kinetic law of a single crystal $(4.3)_4$ can be written in the form

$$\tau^{(\nu)} = \left[\tau_c^{(\nu)} + \boldsymbol{\kappa}^{(\nu)} : \boldsymbol{\tau}\right] \{1 + \Phi^{-1}[T^{(\nu)}\dot{\gamma}^{(\nu)}]\}. \tag{5.1}$$

When the relaxation time $T^{(\nu)} = 0$, then (5.1) gives

$$\tau^{(\nu)} = \tau_c^{(\nu)}(\gamma, \vartheta, \beta, \xi) + \boldsymbol{\kappa}^{(\nu)} : \boldsymbol{\tau}. \tag{5.2}$$

Material differentiation of (5.2) yields

$$\dot{\gamma}^{(\nu)} = \sum_{\delta=1}^{n} \hat{h}_{\nu\delta}^{-1}(\dot{\tau}^{(\delta)} + \boldsymbol{\kappa}^{(\delta)} : \dot{\boldsymbol{\tau}}) + \pi^{(\nu)}\dot{\vartheta} - \sum_{\delta=1}^{n} g_{\nu\delta}\dot{\beta}^{(\delta)} - \sum_{\delta=1}^{n} l_{\nu\delta}\dot{\xi}^{(\delta)}, \tag{5.3}$$

where

$$\hat{h}_{\nu\delta} = \frac{\partial \tau_c^{(\nu)}}{\partial \gamma^{(\delta)}}, \quad \pi^{(\nu)} = -\sum_{\delta=1}^{n} \frac{\partial \tau_c^{(\delta)}}{\partial \vartheta} \hat{h}_{\nu\delta}^{-1},$$

(5.4)

$$g_{\nu\delta} = \sum \frac{\partial \tau_c^{(\nu)}}{\partial \beta^{(\delta)}} \hat{h}_{\nu\delta}^{-1}, \quad l_{\nu\delta} = \sum_{\delta=1}^{n} \frac{\partial \tau_c^{(\nu)}}{\partial \zeta^{(\delta)}} \hat{h}_{\nu\delta}^{-1}.$$

We interpret $\hat{h}_{\nu\delta}^{-1}$ as the modulus hardening rate matrix, $\pi^{(\nu)}$ as the thermal plastic softening coefficient, $g_{\nu\delta}$ as the dislocation obstacle hardening matrix, and $l_{\nu\delta}$ as the point defect hardening matrix.

Equation (5.3) constitutes the fundamental evolution equation for shearing $\gamma^{(\nu)}$ in elastic-plastic rate-independent response of single crystals.

6. Adiabatic process

6.1. *Discussion of cooperative phenomena*

For adiabatic process ($\mathbf{q} = 0$) Eq. (4.13) takes the form

$$(\rho c_p - \lambda)\dot{\vartheta} = \vartheta \frac{\rho}{\rho_{Ref}} \frac{\partial \boldsymbol{\tau}}{\partial \vartheta} : \mathbf{d} + \chi \boldsymbol{\tau} : \mathbf{d}^p + \sum_{\delta=1}^{n} \sum_{\kappa=1}^{n} \Lambda^{(\delta\kappa)} \tau^{(\delta)} \dot{\gamma}^{(\kappa)}. \tag{6.1}$$

The first term on the right-hand side of Eq. (6.1) is not dissipative and is of the second order when compared with the internal dissipation terms. Its contribution to internal heating is small. This suggests that it can be neglected in some considerations like the adiabatic shear-band formation. However, this nondissipative term can have important influence on the propagation of acceleration waves in an inelastic crystal.

When the nondissipative term is neglected, then Eq. (6.1) takes the form

$$(\rho c_p - \lambda)\dot{\vartheta} = \chi \boldsymbol{\tau} : \mathbf{d}^p + \sum_{\delta=1}^{n} \sum_{\kappa=1}^{n} \Lambda^{(\delta\kappa)} \tau^{(\delta)} \dot{\gamma}^{(\kappa)}. \tag{6.2}$$

From Eq. (6.2) we can compute the irreversibility coefficient χ. It gives

$$\chi = \frac{(\rho c_p - \lambda)\dot{\vartheta} - \sum_{\delta=1}^{n} \sum_{\kappa=1}^{n} \Lambda^{(\delta\kappa)} \tau^{(\delta)} \dot{\gamma}^{(\kappa)}}{\boldsymbol{\tau} : \mathbf{d}^p}. \tag{6.3}$$

For $\lambda = 0$ and $\Lambda^{(\delta k)} = 0$, i.e. when the influence of the evolution of the dislocation substructure is not taken into consideration, Eq. (6.3) takes the form

$$\chi = \frac{\rho c_p \dot{\vartheta}}{\boldsymbol{\tau} : \mathbf{d}^p}. \tag{6.4}$$

For this particular case the irreversibility coefficient χ has a simple interpretation as the heat-rate conversion to plastic work-rate fraction. However, Eq. (6.3) shows that the remaining work rate is attributed to the stored energy, e.g. dislocations, point defects and their interactions and is described by two additional terms, namely by $\lambda\dot{\vartheta}$ and $\sum_{\delta=1}^{n} \sum_{\nu=1}^{n} \Lambda^{(\delta\nu)} \tau^{(\delta)} \dot{\gamma}^{(\nu)}$.

Let us denote the rate of the stored energy by

$$s = \lambda\dot{\vartheta} + \sum_{\delta=1}^{n} \sum_{\nu=1}^{n} \Lambda^{(\delta\nu)} \tau^{(\delta)} \dot{\gamma}^{(\nu)}, \tag{6.5}$$

then the irreversibility coefficient χ (cf. Eq. (6.3)) takes the form

$$\chi = \frac{\rho c_p \dot{\vartheta} - s}{\boldsymbol{\tau} : \mathbf{d}^p} \tag{6.6}$$

and Eq. (6.1) can be written as follows:

$$\rho c_p \dot{\vartheta} = \vartheta \frac{\rho}{\rho_{Ref}} \frac{\partial \boldsymbol{\tau}}{\partial \vartheta} : \mathbf{d} + \chi \boldsymbol{\tau} : \mathbf{d}^p + s. \tag{6.7}$$

Let us define a sum of all dissipative terms in Eq. (6.7) by

$$w = \chi \boldsymbol{\tau} : \mathbf{d}^p + \lambda \dot{\vartheta} + \sum_{\delta=1}^{n} \sum_{\nu=1}^{n} \Lambda^{(\delta\nu)} \tau^{(\delta)} \dot{\gamma}^{(\nu)}. \tag{6.8}$$

After WILLEMS [70] and GURTIN [25] we can define the storage function

$$S(t) = S(0) + \int_0^t w(z) dz. \tag{6.9}$$

The storage function (6.9) plays a fundamental role in the determination of stability criteria for dynamic plastic flow processes in single crystals. It takes account of the most important cooperative phenomena coupled with thermal effects[6].

When modelling thermomechanical behaviour of materials, χ is usually assumed to be a constant in the range $0.85 - 0.95$ (a practice that dates back to the work of TAYLOR and QUINNEY [66]).

Recent experimental investigations performed by MASON *et al.* [38] by using a Kolsky (split Hopkinson) pressure bar and a high-speed infrared detector array have clearly shown that this assumption may not be correct for all metals, cf. Fig. 14.

The reason for this considerable discrepancy is clearly visible from Eq. (6.6). The rate of the stored energy s implied by the evolution of the dislocation substructure is responsible for reduction χ (e.g. as it has been observed for Ti-6Al-4V deformed at high strain-rates, that χ decreases from 0.975 to 0.5, cf. Fig. 14).

MASON *et al.* [38] observed that the irreversibility coefficient χ depends on strain and strain-rate in a range of metals. Their experimental observations have significant implications in the study of the conditions preceding and governing adiabatic shear-band formation and shear-band growth as well as on the establishment of a criterion governing dynamic fracture mode selection in rate-sensitive materials.

6.2. General formulation

To investigate the behaviour of rate-dependent elasto-plastic single crystal during an adiabatic dynamic process and particularly, to examine the shear-band formation, let us formulate the initial boundary value problem as follows.

[6] For general methods of the description of cooperative phenomena and synergetic effects see GLONSDORFF and PRIGOGINE [21], NICOLIS and PRIGOGINE [44] and HAKEN [27, 28, 29].

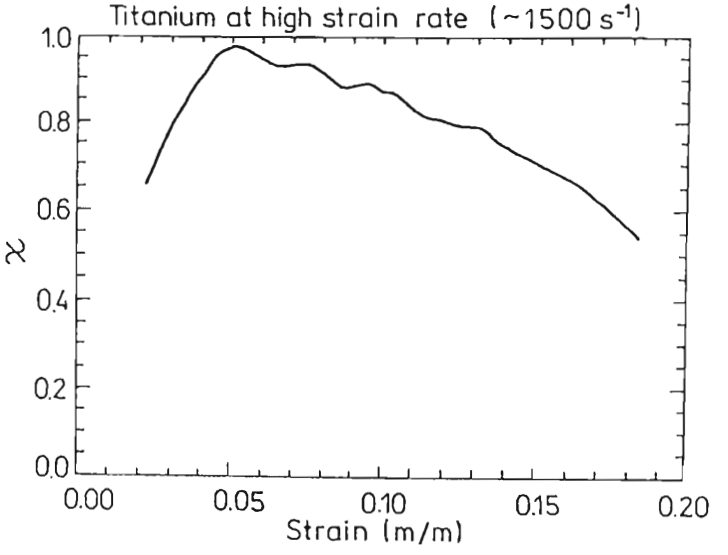

FIG. 14. The irreversibility coefficient χ versus strain calculated for Ti-6Al-4V titanium using the average of the temperature of the two detectors (after Mason *et al.* [38]).

Find ϕ, $\boldsymbol{v}$, ρ, $\boldsymbol{\tau}$, $\gamma^{(\nu)}$, $\alpha^{(\nu)}$, $\beta^{(\nu)}$, $\xi^{(\nu)}$ and ϑ as functions of t and $\mathbf{x}$ such that the following assertions are satisfied:

(i) the field equations

$$
\begin{aligned}
\dot{\phi} &= \boldsymbol{v}, \\
\dot{\boldsymbol{v}} &= \frac{1}{\rho}\mathrm{div}\left(\frac{1}{J}\boldsymbol{\tau}\right), \\
\dot{\rho} &= \rho \mathrm{div}\boldsymbol{v}, \\
\mathrm{L}_{\boldsymbol{v}}\boldsymbol{\tau} &= \mathcal{L}^{e} : \mathbf{d} - \mathcal{L}^{th}\dot{\vartheta} - \sum_{\nu=1}^{n}[\mathcal{L}^{e} : \mathbf{N}^{(\nu)} + \mathbf{b}^{(\nu)}]\dot{\gamma}^{(\nu)}, \\
\dot{\gamma}^{(\nu)} &= \frac{1}{T^{(\nu)}}\langle \Phi\left[\frac{\tau^{(\nu)}}{\tau_{c}^{(\nu)}(\gamma,\beta,\xi,\vartheta) + \boldsymbol{\kappa}^{(\nu)} : \boldsymbol{\tau}} - 1\right]\rangle \mathrm{sgn}\tau^{(\nu)}, \qquad (6.10) \\
\dot{\alpha}^{(\nu)} &= \sum_{\delta=1}^{n} A_{1}^{(\nu\delta)}\dot{\gamma}^{(\delta)} + A_{2}^{(\nu)}\dot{\vartheta}, \\
\dot{\beta}^{(\nu)} &= \sum_{\delta=1}^{n} B_{1}^{(\nu\delta)}\dot{\gamma}^{(\delta)} + B_{2}^{(\nu)}\dot{\vartheta}, \\
\dot{\xi}^{(\nu)} &= \sum_{\delta=1}^{n} C_{1}^{(\nu\delta)}\dot{\gamma}^{(\delta)} + C_{2}^{(\nu)}\dot{\vartheta},
\end{aligned}
$$

$$\dot{\vartheta} = \frac{1}{\rho c_p - \lambda}\left[\vartheta \frac{\rho}{\rho_{Ref}} \frac{\partial \boldsymbol{\tau}}{\partial \vartheta} : \mathbf{d} + \chi \boldsymbol{\tau} : \mathbf{d}^p + \sum_{\nu=1}^{n}\sum_{\delta=1}^{n} \Lambda^{(\nu\delta)} \tau^{(\nu)} \dot{\gamma}^{(\delta)}\right]; \tag{6.10 [cont.]}$$

(ii) the boundary conditions

(a) displacement ϕ is prescribed on a part ∂_ϕ of $\partial\phi(\mathcal{B})$ and tractions $(\boldsymbol{\tau} \cdot \mathbf{n})^a$ are prescribed on part $\partial_{\boldsymbol{\tau}}$ of $\partial\phi(\mathcal{B})$, where $\partial_\phi \cap \partial_{\boldsymbol{\tau}} = 0$ and $\overline{\partial_\phi \cup \partial_{\boldsymbol{\tau}}} = \partial\phi(\mathcal{B})$;

(b) heat flux $(\mathbf{q} \cdot \mathbf{n}) = 0$ is prescribed on $\partial\phi(\mathcal{B})$;

(iii) the initial conditions: ϕ, $\boldsymbol{v}$, ρ, $\boldsymbol{\tau}$, $\gamma^{(\nu)}$, $\alpha^{(\nu)}$, $\beta^{(\nu)}$, $\xi^{(\nu)}$ and ϑ are given at $X \in \mathcal{B}$ at $t = 0$.

For elasto-plastic rate-independent response of crystals, to define an adiabatic flow process, we have to replace Eq. $(6.10)_5$ by Eq. (5.3).

6.3. Rate-dependent process

For an adiabatic process, the rate equation for temperature $(6.10)_9$ can be written in the form

$$\dot{\vartheta} = \mathcal{F} : \mathbf{d} + \sum_{\nu=1}^{n} K^{(\nu)} \dot{\gamma}^{(\nu)} \tag{6.11}$$

where

$$\begin{aligned} \mathcal{F} &= \frac{\rho}{\rho_{Ref}} \frac{\vartheta}{(\rho c_p - \lambda)} \frac{\partial \boldsymbol{\tau}}{\partial \vartheta}, \\ K^{(\nu)} &= \frac{1}{\rho c_p - \lambda}\left[\chi \tau^{(\nu)} + \sum_{\delta=1}^{n} \Lambda^{(\delta\nu)} \tau^{(\delta)}\right]. \end{aligned} \tag{6.12}$$

Let us denote

$$P^{(\delta)} = \frac{1}{T^{(\delta)}} \langle \Phi\left[\frac{\tau^{(\delta)}}{\tau_c^{(\delta)} + \boldsymbol{\kappa}^{(\delta)} : \boldsymbol{\tau}} - 1\right]\rangle \operatorname{sgn} \tau^{(\delta)}, \tag{6.13}$$

then the evolution equations $(6.10)_{6-8}$ take the form as follows:

$$\begin{aligned} \dot{\alpha}^{(\nu)} &= \sum_{\delta=1}^{n}\left(A_1^{(\nu\delta)} + A_2^{(\nu)} K^{(\delta)}\right) P^{(\delta)} + A_2^{(\nu)} \mathcal{F} : \mathbf{d}, \\ \dot{\beta}^{(\nu)} &= \sum_{\delta=1}^{n}\left(B_1^{(\nu\delta)} + B_2^{(\nu)} K^{(\delta)}\right) P^{(\delta)} + B_2^{(\nu)} \mathcal{F} : \mathbf{d}, \\ \dot{\xi}^{(\nu)} &= \sum_{\delta=1}^{n}\left(C_1^{(\nu\delta)} + C_2^{(\nu)} K^{(\delta)}\right) P^{(\delta)} + C_2^{(\nu)} \mathcal{F} : \mathbf{d}. \end{aligned} \tag{6.14}$$

The fundamental rate equation for the Kirchhoff stress $(6.10)_4$ takes the form

$$\mathrm{L}_{\boldsymbol{v}}\boldsymbol{\tau} = \mathbb{E} : \mathbf{d} + \mathbb{F}, \tag{6.15}$$

where

$$\begin{aligned} \mathbb{E} &= \mathcal{L}^e - \frac{\rho}{\rho_{Ref}} \frac{\vartheta}{(\rho c_p - \lambda)} \mathcal{L}^{th} \frac{\partial \boldsymbol{\tau}}{\partial \vartheta}, \\ \mathbb{F} &= -\sum_{\nu=1}^{n} \left(\mathcal{L}^e : \mathbf{N}^{(\nu)} + \mathbf{b}^{(\nu)} + \mathcal{L}^{th} K^{(\nu)} \right) P^{(\nu)}. \end{aligned} \tag{6.16}$$

6.4. Rate-independent process

Taking into account the equation for $\dot{\tau}^{(\nu)}$ (cf. DUSZEK-PERZYNA and PERZYNA [15], Eq. (46))

$$\dot{\tau}^{(\nu)} = \mathbf{Q}^{(\nu)} : \mathbf{d} - \mathbf{Q}^{(\nu)} : \sum_{\delta=1}^{n} \mathbf{N}^{(\delta)} \dot{\gamma}^{(\delta)} - \mathcal{L}^{th} : \mathbf{N}^{(\nu)} \dot{\vartheta} \tag{6.17}$$

where

$$\mathbf{Q}^{(\nu)} = \mathcal{L}^e : \mathbf{N}^{(\nu)} + \mathbf{b}^{(\nu)}, \tag{6.18}$$

and the evolution equation (2.8) and (6.11), we obtain

$$\begin{aligned} \dot{\gamma}^{(\nu)} = \sum_{\delta=1}^{n} M^{-1}_{(\nu\delta)} \Bigg[\mathbf{Q}^{(\delta)} - \Bigg(\mathcal{L}^{th} : \mathbf{N}^{(\delta)} + \frac{\partial \tau_c^{(\delta)}}{\partial \vartheta} \\ + \sum_{\kappa=1}^{n} \frac{\partial \tau_c^{(\delta)}}{\partial \beta^{(\kappa)}} B_2^{(\kappa)} + \sum_{\kappa=1}^{n} \frac{\partial \tau_c^{(\delta)}}{\partial \xi^{(\kappa)}} C_2^{(\kappa)} \Bigg) \mathcal{F} - \boldsymbol{\kappa}^{(\delta)} : \mathcal{L}^e \Bigg] : \mathbf{d} \end{aligned} \tag{6.19}$$

where

$$\begin{aligned} M_{(\nu\delta)} = h_{\nu\delta} + \mathbf{Q}^{(\nu)} : \mathbf{N}^{(\delta)} + \left(\mathcal{L}^{th} : \mathbf{N}^{(\nu)} + \frac{\partial \tau_c^{(\nu)}}{\partial \vartheta} \right) K^{(\delta)} \\ + \sum_{\kappa=1}^{n} \left[\frac{\partial \tau_c^{(\nu)}}{\partial \beta^{(\kappa)}} \left(B_1^{(\kappa\delta)} + B_2^{(\kappa)} K^{(\delta)} \right) + \frac{\partial \tau_c^{(\nu)}}{\partial \xi^{(\kappa)}} \left(C_1^{(\kappa\delta)} + C_2^{(\kappa)} K^{(\delta)} \right) \right] \\ - \boldsymbol{\kappa}^{(\nu)} : \mathcal{L}^e : \mathbf{N}^{(\delta)}. \end{aligned} \tag{6.20}$$

Substituting (6.19) and (6.11) into $(6.10)_4$ yields

$$\mathrm{L}_{\boldsymbol{v}}\boldsymbol{\tau} = \mathbb{L} : \mathbf{d} \tag{6.21}$$

where the fundamental matrix $\mathbb{L}$ has the following form:

$$\mathbb{L} = \mathcal{L}^e - \mathcal{L}^{th}\mathcal{F} - \sum_{\nu=1}^{n}\sum_{\delta=1}^{n}\left(\mathbf{Q}^{(\nu)} + \mathcal{L}^{th}K^{(\nu)}\right)M^{-1}_{(\nu\delta)}\left\{\mathbf{Q}^{(\delta)} - \left[\mathcal{L}^{th} : \mathbf{N}^{(\delta)} + \frac{\partial \tau_c^{(\delta)}}{\partial \vartheta} + \sum_{\kappa=1}^{n}\left(\frac{\partial \tau_c^{(\delta)}}{\partial \beta^{(\kappa)}}B_2^{(\kappa)} + \frac{\partial \tau_c^{(\delta)}}{\partial \xi^{(\kappa)}}C_2^{(\kappa)}\right)\right]\mathcal{F} - \boldsymbol{\kappa}^{(\delta)} : \mathcal{L}^e\right\}. \tag{6.22}$$

7. Analysis of acceleration waves

7.1. General considerations

To investigate the intrinsic mathematical structure of the set of the field equations (6.10) which determine the adiabatic inelastic flow processes, let us analyse the problem of propagation of acceleration waves. We shall show that the theory of acceleration waves in the materials considered can be based on the notion of an instantaneous adiabatic acoustic tensor.

Let $\sum(t)$ denote a smooth surface with outward normal $\mathbf{n}$ which is moving through the solid body with velocity $\mathbf{w}(t, \mathbf{x})$. Some field quantities or their derivatives may be discontinuous across $\sum(t)$ which is then called a singular surface. If the surface $\sum(t)$ is composed of the same material points at all times, one then refers to $\sum(t)$ as a stationary discontinuity. Otherwise, the surface $\sum(t)$ is called a propagating singular surface or wave, cf. Hill [30].

Let c denote the normal speed of propagation of $\sum(t)$ with respect to the material in its current configuration. It is related to the spatial velocity $\boldsymbol{v}(t, \mathbf{x})$ and to the normal wave speed $w = \mathbf{w} \cdot \mathbf{n}$, by the following equation:

$$c = w - \boldsymbol{v} \cdot \mathbf{n}. \tag{7.1}$$

It is said that $\sum(t)$ is an acceleration wave if the fields ϕ, $\boldsymbol{v}$, $\mathbf{F}$, $\boldsymbol{\mu}$ and ϑ are continuous functions of t and $\mathbf{x}$, while $\dot{\boldsymbol{v}}$, $\nabla\boldsymbol{v}$, $\dot{\mathbf{F}}$, $\nabla\mathbf{F}$, $\dot{\boldsymbol{\mu}}$, $\nabla\boldsymbol{\mu}$, $\dot{\vartheta}$, $\nabla\vartheta$ have (at most) jump discontinuities across $\sum(t)$ but are continuous in t and $\mathbf{x}$ jointly everywhere else ($\boldsymbol{\mu}$ denotes a set of the internal state variables).

An acceleration wave in which $\dot{\vartheta}$ and $\nabla\vartheta$ are continuous functions of t and $\mathbf{x}$ is called homothermal.

From the definition of an acceleration wave and the constitutive assumption $\psi = \hat{\psi}(\mathbf{e}, \mathbf{F}, \vartheta, \gamma^{(\alpha)})$ we have

$$[\![\psi]\!] = [\![\boldsymbol{\sigma}]\!] = [\![\eta]\!] = 0, \tag{7.2}$$

where $[\![\cdot]\!]$ denotes the jump of a quantity across $\sum(t)$ in the direction of its local normal $\mathbf{n}(t, \mathbf{x})$.

Hadamard's compatibility conditions require the jumps in velocity and stress derivatives to be related as follows (cf. HADAMARD [26]):

$$[\![\nabla \boldsymbol{v}]\!] = -\frac{1}{c}[\![\mathbf{a}]\!]\,\mathbf{n}, \tag{7.3}$$

$$[\![\nabla \boldsymbol{\sigma}]\!] = -\frac{1}{c}[\![\dot{\boldsymbol{\sigma}}]\!]\,\mathbf{n},$$

where ∇ denotes the spatial gradient and $\mathbf{a} = \dot{\boldsymbol{v}}$.

Balance of momentum requires that (cf. $(6.10)_2$)

$$\operatorname{div}\boldsymbol{\sigma} = \rho\,\mathbf{a}. \tag{7.4}$$

Combining $(7.3)_2$ and (7.4) yields

$$\mathbf{n}\cdot[\![\dot{\boldsymbol{\sigma}}]\!] = -\rho c\,[\![\mathbf{a}]\!]. \tag{7.5}$$

From the last result it becomes clear that the existence and propagation speed of acceleration waves in solids is directly related to the assumed constitutive structure of the material.

Since ϑ is continuous across $\sum(t)$, we have

$$[\![\dot{\vartheta}]\!] = -c\,[\![\nabla\vartheta]\!]\cdot\mathbf{n}. \tag{7.6}$$

For an acceleration wave in an adiabatic process we have (cf. PERZYNA [50])

$$[\![\mathbf{q}]\!] = 0, \qquad [\![\dot{\mathbf{q}}]\!] = 0 \tag{7.7}$$

and

$$[\![\dot{\vartheta}]\!] \neq 0, \qquad [\![\nabla\vartheta]\!] \neq 0. \tag{7.8}$$

Hence an acceleration wave in inelastic solids for an adiabatic process is not homothermal.

This conclusion will play an important role in the analysis of acceleration waves in particular material models for adiabatic process of a crystal.

7.2. Rate-dependent adiabatic process

Since $\mathbb{F}$ is continuous across $\sum(t)$ Eq. (6.15) gives

$$[\![\mathrm{L}_{\boldsymbol{v}}\boldsymbol{\tau}]\!] = \mathbb{E} : [\![\mathbf{d}]\!]. \tag{7.9}$$

Combining Eqs. $(7.3)_1$, (7.5) and (7.9) we can prove

THEOREM 1: *For an adiabatic rate-dependent plastic flow process of a single crystal described by Eqs. (6.10), the acceleration discontinuity* $[\![\mathbf{a}]\!]$ *is the solution of the eigenvalue problem*

$$\mathbf{A} \cdot [\![\mathbf{a}]\!] = \rho_{Ref} c^2 [\![\mathbf{a}]\!], \tag{7.10}$$

where

$$\mathbf{A} = \mathbf{n} \cdot (I\!E \cdot \mathbf{n} + \boldsymbol{\tau} \cdot \mathbf{ng}) \tag{7.11}$$

denotes the instantaneous adiabatic acoustic tensor.

It is noteworthy to stress that the instantaneous adiabatic acoustic tensor $\mathbf{A}$ for rate-dependent response of a single crystal does depend on the evolution of the dislocation substructure. This is implied by the direct dependence of the adiabatic matrix $I\!E$ on the coefficient λ.

Let us assume the strong ellipticity condition in the form

$$I\!E^{abcd} \zeta_a \zeta_c \mu_b \mu_d \geq \epsilon \|\boldsymbol{\zeta}\|^2 \|\boldsymbol{\mu}\|^2 \tag{7.12}$$

for all vectors $\boldsymbol{\zeta}$ and $\boldsymbol{\mu} \in I\!R^3$.

Then we can prove that all eigenvalues of the acoustic tensor $\mathbf{A}$ are real and positive.

Thus, the Cauchy problem

$$\dot{\boldsymbol{\varphi}} = \mathcal{A}(t, \boldsymbol{\varphi})\boldsymbol{\varphi} + \mathbf{f}(t, \boldsymbol{\varphi}), \quad t \in [0, t_f], \quad \boldsymbol{\varphi}(0, \mathbf{x}) = \boldsymbol{\varphi}^0(\mathbf{x}), \tag{7.13}$$

for the field equations (6.10) is well-posed provided some conditions for the spatial differential operator $\mathcal{A}$ and the nonlinear function $\mathbf{f}$ are satisfied[7]. This fact has very important implications for the numerical simulation of an adiabatic inelastic flow process.

It can be proved that the localization of plastic deformation in an elastic-viscoplastic crystal body may arise only as the result of the interaction and reflection of stress waves. It has a different character than that which occurs in a rate-independent elasto-plastic single crystal.

Viscosity introduces implicitly a length-scale parameter into the dynamical initial-boundary value problem and hence, it implies that the localized shear-band region is diffused when compared with that in an inviscid plastic material. Rate dependency (viscosity) allows the spatial difference operator in the governing equations to retain its ellipticity and the initial value problem is well-posed.

Since the rate-independent plastic response is obtained as the limit case when the relaxation time T tends to zero, hence the theory of viscoplasticity offers the regularization procedure for the solution of the dynamical initial-boundary value problems with localization of plastic deformation.

[7] For a discussion of the well-posedness of the Cauchy problem see PERZYNA [50].

7.3. Rate-independent adiabatic process

Combining Eqs. $(7.3)_1$, (7.5) and (6.21) we can prove

THEOREM 2: *For an adiabatic rate-independent plastic flow process of a single crystal described by Eqs. $(6.10)_{1-4}$ and $(6.10)_{6-9}$ and (5.3), the acceleration discontinuity $[\![\mathbf{a}]\!]$ is the solution of the eigenvalue problem*

$$\hat{\mathbf{A}} \cdot [\![\mathbf{a}]\!] = \rho_{Ref} c^2 [\![\mathbf{a}]\!], \tag{7.14}$$

where

$$\hat{\mathbf{A}} = \mathbf{n} \cdot (I\!I\!L \cdot \mathbf{n} + \boldsymbol{\tau} \cdot \mathbf{ng}) \tag{7.15}$$

denotes the instantaneous adiabatic acoustic tensor.

8. MACROSCOPIC ADIABATIC SHEAR-BAND FORMATION

8.1. Necessary conditions

Let us denote $\lambda = \rho_{Ref} c^2$, then the eigenvalue problem (7.14) takes the form

$$\hat{\mathbf{A}} \cdot [\![\mathbf{a}]\!] = \lambda [\![\mathbf{a}]\!]. \tag{8.1}$$

The necessary and sufficient condition for (8.1) to have a non-trivial solution is

$$\det[\hat{\mathbf{A}} - \lambda I\!I] = 0, \tag{8.2}$$

where $I\!I$ is the 3×3 unit matrix.

When zero is an eigenvalue of the instantaneous adiabatic acoustic tensor $\hat{\mathbf{A}}$, then the associated discontinuity does not propagate ($c = 0$) and we speak of a stationary discontinuity. In a quasi-static case this situation is referred to as the strain localization condition. It corresponds to a loss of hyperbolicity of the dynamical equations.

To satisfy this condition let us assume $\lambda = 0$ in Eq. (8.2). Then the necessary condition for a localized plastic deformation region to be formed is as follows

$$\det \hat{\mathbf{A}} = 0. \tag{8.3}$$

It is noteworthy that this condition for localization is equivalent to that obtained by using the standard bifurcation method (cf. RICE [58], RUDNICKI and RICE [59], DUSZEK and PERZYNA [13], DUSZEK *et al.* [16]).

In what follows we shall neglect the influence of the point defects, i.e. we assume $\dot{\xi} = 0$ and $\xi_0 = 0$. It means that we concentrate only on the interaction of the thermally activated and phonon damping mechanisms in the case when the concentration of the point defects can be neglected, e.g. for the mechanism of the intersection of forest dislocations, cf. Fig 9(i).

8.2. Necessary conditions for symmetric double slip process

Let us introduce the Cartesian coordinate system $\{x^i\}$. To obtain the direct analytical results we shall introduce the following simplifications:

(i) Let us assume

$$\mathbf{Z} = \mathbf{s} \cdot (\mathbf{s} \cdot \mathcal{L}^e). \tag{8.4}$$

(ii) Let us restrict our consideration to the linear, isotropic and homogeneous elastic properties of the crystal, i.e.

$$(\mathcal{L}^e)^{abcd} = \tau^{bd} g^{ac} + \mu(g^{ac} g^{bd} + g^{ad} g^{bc}) + \lambda g^{ab} g^{cd}, \tag{8.5}$$

where the constants μ and λ are the Lamé moduli.
The localization condition (8.3) gives the result as follows (cf. PERZYNA and KORBEL [54]):

$$A\left(\frac{n_1}{n_2}\right)^4 + B\left(\frac{n_1}{n_2}\right)^3 + C\left(\frac{n_1}{n_2}\right)^2 + D\left(\frac{n_1}{n_2}\right) + E = 0, \tag{8.6}$$

where

$$\begin{aligned}
A &= (\mathbb{L}^{2222} + \tau^{22})(\mathbb{L}^{2112} + \tau^{22}),\\
B &= (\mathbb{L}^{2222} + \tau^{22})(\mathbb{L}^{1112} + \mathbb{L}^{2111}) + (\mathbb{L}^{2112} + \tau^{22})(\mathbb{L}^{1222} + \mathbb{L}^{2221})\\
&\quad - \mathbb{L}^{2212}(\mathbb{L}^{1122} + \mathbb{L}^{2121}),\\
C &= (\mathbb{L}^{1111} + \tau^{11})(\mathbb{L}^{2222} + \tau^{22}) + (\mathbb{L}^{1222} + \mathbb{L}^{2221})(\mathbb{L}^{1112} + \mathbb{L}^{2111})\\
&\quad + (\mathbb{L}^{1221} + \tau^{11})(\mathbb{L}^{2112} + \tau^{22}) - (\mathbb{L}^{1122} + \mathbb{L}^{2121})(\mathbb{L}^{1212} + \mathbb{L}^{2211})\\
&\quad - \mathbb{L}^{1121}\mathbb{L}^{2212},\\
D &= (\mathbb{L}^{1111} + \tau^{11})(\mathbb{L}^{1222} + \mathbb{L}^{2221}) + (\mathbb{L}^{1221} + \tau^{11})(\mathbb{L}^{1112} + \mathbb{L}^{2111})\\
&\quad - \mathbb{L}^{1121}(\mathbb{L}^{1212} + \mathbb{L}^{2211}),\\
E &= (\mathbb{L}^{1111} + \tau^{11})(\mathbb{L}^{1221} + \tau^{11}).
\end{aligned} \tag{8.7}$$

The ratio $\frac{n_2}{n_1} = \tan\beta$ determines the direction of the shear-band. The localization of plastic deformations along the shear-band may take place if real $\mathbf{n}$ exist.

When the evolution of substructure and the non-Schmid effects are not taken into consideration, then the fundamental matrix $\mathbb{L}$ takes the form which has been first considered by DUSZEK-PERZYNA and PERZYNA [15]. When additionally the Lie derivative is replaced by the Zaremba-Jaumann rate and an isothermal

process is assumed, then the fundamental matrix $\mathbb{L}$ is the same as that which has been considered by PEIRCE *et al.* [46].

For symmetric double slip process it is assumed that the crystal has two active slip plane (primary and conjugate) systems, symmetrically oriented with respect to the maximum principal stress τ^{22} (the tensile axis is x^2) direction at the angle φ, cf. Fig. 15. Then the subscripts ν and δ take on values 1 and 2.

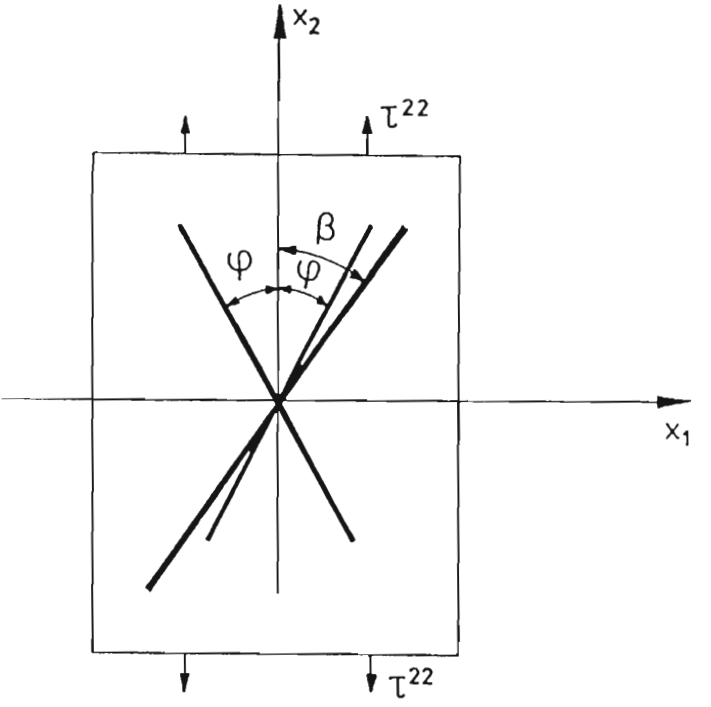

FIG. 15. Schematic representation of symmetric primary-conjugate double slip systems of single crystals.

Let us assume further that

$$h_{11} = h_{22} = h, \quad h_{12} = h_{21} = h_1, \quad q = \frac{h_1}{h} \quad \tau_c^{(1)} = \tau_c^{(2)} = \tau_c,$$

$$\alpha^{(1)} = \alpha^{(2)} = \alpha, \quad \beta^{(1)} = \beta^{(2)} = \beta,$$

$$\boldsymbol{\kappa}^{(1)} = \boldsymbol{\kappa}^{(2)} = \begin{bmatrix} 0 & \frac{1}{2}\kappa \\ \frac{1}{2}\kappa & 0 \end{bmatrix}, \quad \kappa \sim O\left(\frac{\tau}{\mathcal{L}^e}\right) \approx 3.48 \cdot 10^{-3}. \tag{8.8}$$

8.3. *Necessary conditions for a single slip process*

A rate-independent constitutive structure of elasto-plastic single crystal in a single slip adiabatic process is described by the equations as follows:

$$
\begin{aligned}
\mathrm{L}_{\boldsymbol{\upsilon}}\boldsymbol{\tau} &= \mathcal{L}^{e} : \mathbf{d} - \mathcal{L}^{th}\dot{\vartheta} - [\mathcal{L}^{e} : \mathbf{N} + \mathbf{b}]\dot{\gamma}, \\
\dot{\gamma} &= \frac{1}{h}(\dot{\tau} + \boldsymbol{\kappa} : \dot{\boldsymbol{\tau}}) + \pi\dot{\vartheta} - g\dot{\beta}, \\
\dot{\alpha} &= a_1\dot{\gamma} + a_2\dot{\vartheta} + a_3\dot{\beta}, \\
\dot{\beta} &= b_1\dot{\gamma} + b_2\dot{\vartheta} + b_3\dot{\alpha}, \\
\dot{\vartheta} &= \frac{1}{\rho c_p}\left[\chi\tau\dot{\gamma} + \chi^{*}\frac{\tau}{a_1}\dot{\alpha} + \chi^{**}\frac{\tau}{b_1}\dot{\beta}\right] + \frac{\vartheta}{\rho_{Ref}c_p}\frac{\partial\boldsymbol{\tau}}{\partial\vartheta} : \mathbf{d},
\end{aligned}
\tag{8.9}
$$

where

$$
h = \frac{\partial\tau_c}{\partial\gamma}, \qquad \pi = -\frac{1}{h}\frac{\partial\tau_c}{\partial\vartheta}, \qquad g = \frac{1}{h}\frac{\partial\tau_c}{\partial\beta}.
\tag{8.10}
$$

Differentiation of the resolved Schmid stress $\tau = \mathbf{s}\cdot\boldsymbol{\tau}\cdot\mathbf{m}$ gives additionally the relation (cf. Eq. (6.17))

$$
\dot{\tau} = [\mathcal{L}^{e} : \mathbf{N} + \mathbf{b}] : (\mathbf{d} - \mathbf{d}^{p}) - \mathcal{L}^{th} : \mathbf{N}\dot{\vartheta}.
\tag{8.11}
$$

Equations (8.9) and (8.11) can be reduced to the fundamental evolution equation as follows:

$$
\mathrm{L}_{\boldsymbol{\upsilon}}\boldsymbol{\tau} = \mathbb{L} : \mathbf{d},
\tag{8.12}
$$

where

$$
\begin{aligned}
\mathbb{L} = \mathcal{L}^{e} - \Theta\frac{\iota}{\Delta}\frac{\mathbf{Z}}{\mu}\frac{\partial\boldsymbol{\tau}}{\partial\vartheta} \\
- \frac{(\mathbf{Q} + \mathcal{L}^{e} : \boldsymbol{\kappa} + \Theta\frac{\tau}{\mu}\mathbf{Z})\left[\mathbf{Q} - \left(\Theta\frac{\mathbf{Z} : \mathbf{N}}{\mu} - \Pi + \Omega\right)\frac{\iota}{\Delta}\frac{\partial\boldsymbol{\tau}}{\partial\vartheta}\right]}{h - \Pi\tau + \Gamma + \Omega\tau + \Theta\frac{\tau}{\mu}\mathbf{Z} : \mathbf{N} + (\mathbf{Q} + \mathcal{L}^{e} : \boldsymbol{\kappa}) : \mathbf{N}},
\end{aligned}
\tag{8.13}
$$

with the notations

$$\mathbf{Q} = \mathcal{L}^e : \mathbf{N} + \mathbf{b}, \qquad \Theta = \Delta\theta\mu, \qquad \theta\mathbf{Z} = \mathcal{L}^{th}, \qquad \Pi = \Delta\pi h,$$
$$\Omega = hg\Delta\frac{b_2 + a_2 b_3}{1 - a_3 b_3}, \qquad \Gamma = hg\frac{b_1 + a_1 b_3}{1 - a_3 b_3},$$

$$\Delta = \frac{\chi(1 - a_3 b_3) + \frac{\chi^*}{a_1}(a_1 + a_3 b_1) + \frac{\chi^{**}}{b_1}(b_1 + a_1 b_3)}{\rho c_p(1 - a_3 b_3) - \frac{\chi^*}{a_1}(a_2 + a_3 b_2) - \frac{\chi^{**}}{b_1}(b_2 + a_2 b_3)}, \tag{8.14}$$

$$\iota = \frac{\vartheta\frac{\rho}{\rho_{Ref}}(1 - a_3 b_3)}{\rho c_p(1 - a_3 b_3) - \frac{\chi^*}{a_1}\tau(a_2 + a_3 b_2) - \frac{\chi^{**}}{b_1}\tau(b_2 + a_2 b_3)}.$$

Let us introduce the Cartesian coordinate system $\{x^i\}$ and restrict to the linear form of $\mathcal{L}^e$ and $\mathbf{Z}$ given by (8.4) and (8.5), respectively.

We shall study the influence of particular effects on adiabatic shear-band localization. First we focus the attention on the discussion of the influence of the evolution of substructure, thermomechanical couplings, non-Schmid effects and covariance terms. This case has been considered by PERZYNA and KORBEL [53, 54]. So, let us neglect in the fundamental matrix $\mathbb{L}$ the nondissipative thermal term effects. Then we have

$$\mathbb{L} = \mathcal{L}^e - \frac{(\mathbf{Q} + \mathcal{L}^e : \boldsymbol{\kappa} + \Theta\frac{\tau}{\mu}\mathbf{Z})\mathbf{Q}}{h - \Pi\tau + \Gamma + \Omega\tau + \Theta\frac{\tau}{\mu}\mathbf{Z} : \mathbf{N} + (\mathbf{Q} + \mathcal{L}^e : \boldsymbol{\kappa}) : \mathbf{N}}. \tag{8.15}$$

Using the necessary condition for localization of plastic deformation (8.3) and applying the perturbation procedure about $\mathbf{n} = \mathbf{m}$, we obtain

$$\mathbf{n} = \mathbf{m} + \left(\frac{\Theta\tau}{2\mu} + \frac{\tau}{4\mu\nu} + \frac{1}{2}\kappa_{ss} + \frac{2\nu - 1}{4\nu}\kappa_{zz}\right)\mathbf{s} + \kappa_{sz}\mathbf{z} + O\left(\frac{\tau}{\mathcal{L}^e}, \frac{\tau^2}{\mathcal{L}^{e2}}\right), \tag{8.16}$$

$$h_{\text{crit}} = \Pi\tau - \Gamma - \Omega\tau + \frac{\tau^2}{\mu}\left(\nu\Theta^2 + \Theta + \frac{1}{4\nu}\right) + \tau(2\nu\Theta + 1)\kappa_{ss}$$
$$+ \tau\left[(2\nu - 1)\Theta + 1 - \frac{1}{2\nu}\right]\kappa_{zz} + \mu\nu(\kappa_{ss})^2 + \frac{\mu(2\nu - 1)^2}{4\nu}(\kappa_{zz})^2$$
$$+ \mu(2\nu - 1)\kappa_{zz}\kappa_{ss} + O\left(\frac{\tau^2}{\mathcal{L}^e}, \frac{\tau^3}{\mathcal{L}^{e2}}\right), \tag{8.17}$$

where

$$\nu = \frac{\lambda + \mu}{\lambda + 2\mu}. \tag{8.18}$$

Now we use the evolution equations for parameters α and β proposed by ESTRIN and KUBIN [17] in the form

$$\begin{aligned} &\dot{\alpha} = a_1(\alpha,\beta)\dot{\gamma}, \qquad a_1(\alpha,\beta) = \frac{c_1}{b^2}\left(\frac{\beta}{\alpha}\right) - c_2\alpha - \frac{c_3}{b}\sqrt{\beta}, \\ &\dot{\beta} = b_1(\alpha,\beta)\dot{\gamma}, \qquad b_1(\alpha,\beta) = c_2\alpha + \frac{c_3}{b}\sqrt{\beta} - c_4\beta, \end{aligned} \tag{8.19}$$

where b is the Burgers vector.

Let us notice that the above equations do not describe the dependence of both densities of dislocations on temperature. Then the considered process is not a fully temperature-dependent process, but it involves temperature only thorough parameter γ. The identification of the coefficients a_1 and b_1 one can find in the paper presented by ESTRIN and KUBIN [17], cf. BASIŃSKI and BASIŃSKI [5].

For the particular case considered by ASARO and RICE [3], when

$$\kappa_{ss} = \kappa_{zz} = 0, \quad \kappa_{zs} = \kappa_{sz} = \frac{1}{2}\kappa, \quad \kappa_{mz} = \kappa_{zm} = \frac{1}{2}\kappa_1, \tag{8.20}$$

we have

$$\mathbf{n} = \mathbf{m} + \left(\frac{\Theta\tau}{2\mu} + \frac{\tau}{4\mu\nu}\right)\mathbf{s} + \frac{1}{2}\kappa\mathbf{z}, \tag{8.21}$$

$$\left(\frac{h}{\tau}\right)_{\text{crit}} = \Pi - \frac{\Gamma}{\tau} + \left(\Theta^2\nu + \Theta + \frac{1}{4\mu}\right)\frac{\tau}{\mu} + \frac{1}{4}\kappa^2\frac{\mu}{\tau}, \tag{8.22}$$

where

$$\begin{aligned} \Theta &= \Delta\theta\mu, \qquad \Pi = \Delta\pi h = -\Delta\frac{\partial\tau_c}{\partial\vartheta}, \\ \Gamma &= b_1\frac{\partial\tau_c}{\partial\beta}, \qquad \Delta = \frac{\chi + \chi^* + \chi^{**}}{\rho c_p}. \end{aligned} \tag{8.23}$$

From estimations of the parameter κ done in paper of ASARO and RICE [3] we have $\kappa = 1.1\sqrt{\dfrac{b}{L}}$ where L is the slip-line length. In the moment of localization we may assume that $L \approx 10^{-6}$ m.

We shall use the experimental data from the papers of CHANG and ASARO [8] for aluminum-copper single crystals tested at 298 K, and SPITZIG [64] for Fe-Ti-Mn single crystals tested at 295 K.

For aluminum-copper single crystals we have the result as follows:

$$\left(\frac{h}{\tau}\right)_{\text{crit}} = 0.043 + 0.0090 + 0.0010 + 0.0032 + 0.0025 + 0.0186 = 0.0773,$$

and for nitrogenated Fe-Ti-Mn crystals

$$\left(\frac{h}{\tau}\right)_{\text{crit}} = 0.0653 + 0.0100 + 0.0012 + 0.004 + 0.003 + 0.0173 = 0.1008.$$

We observe that the non-Schmid effects are about three times smaller than the thermal plastic softening effects Π, and about two times larger than the interaction between macro- and microstructure $\dfrac{\Gamma}{\tau_{\text{crit}}}$.

9. Discussion of the synergetic effects and comparison with experimental observations

We shall consider both the single slip and symmetric double slip processes. All numerical results are taken from the paper by Perzyna and Korbel [54].

9.1. Single slip process

For a single slip process, numerical computations have been performed for the fundamental matrix $\mathbb{L}$ determined by Eq. (8.15) by using the necessary condition (8.3).

For Al-Cu single crystals some particular material parameters are taken from Chang and Asaro [8]. We consider the same example of uniaxial tension as that tested by Chang and Asaro [8] at room temperature. The results obtained for the hardening modulus rate h/τ^{22} as a function of the misalignment angle δ are plotted in Fig. 16.

For nitrogenated Fe-Ti-Mn single crystals, some particular material parameters are taken from Spitzig's [64] experimental data. The same example as that tested by Spitzig [64] at room temperature (295 K) has been considered. The results obtained for the hardening modulus rate h/τ^{22} as a function of the misalignment angle δ are presented in Fig. 17.

9.2. Symmetric double slip process

For symmetric double slip process, numerical computations have been performed for the fundamental matrix $\mathbb{L}$ determined by Eq. (6.22) with simplifying assumptions (8.4), (8.5), (8.8), and by using the necessary condition (8.6).

For Al-Cu single crystals an example of uniaxial tension has been considered at room temperature with the orientation as follows: $s_1 = (\bar{1}, 0, 1)$, $m_1 = [\bar{1}, \bar{1}, 1]$

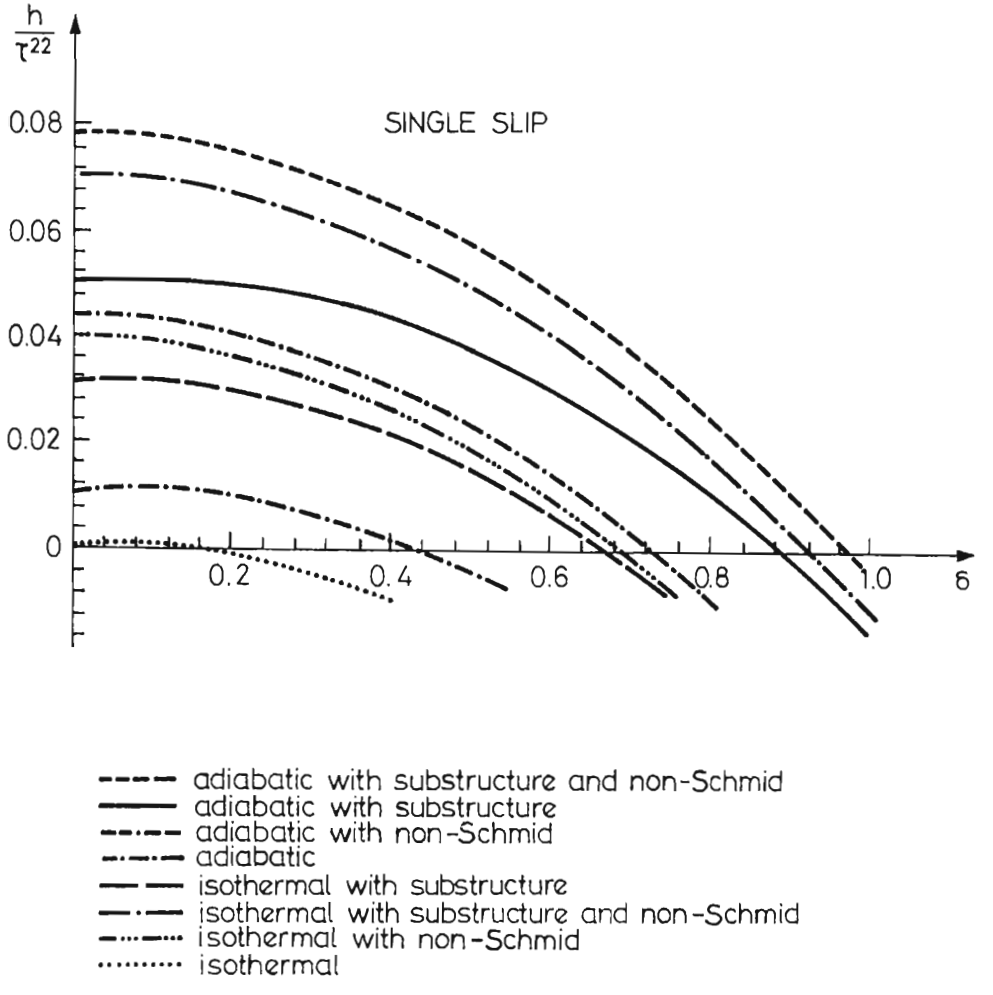

FIG. 16. Numerical results for single slip process for the hardening modulus rate h/τ^{22} as function of the misalignment angle δ for Al-Cu single crystal.

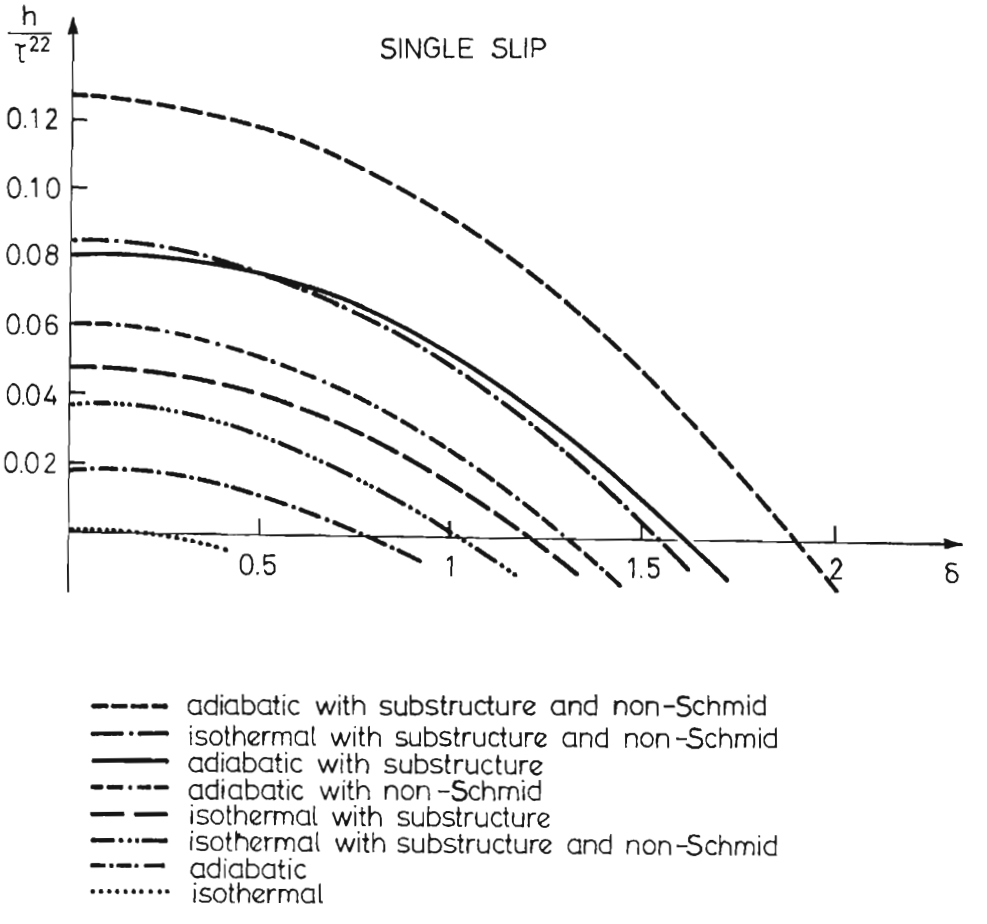

FIG. 17. Numerical results for single slip process for the hardening modulus rate h/τ^{22} as function of the misalignment angle δ for Fe-Ti-Mn single crystal

and $s_2 = (0,1,1)$, $m_2 = [\bar{1},\bar{1},1]$. The numerical results obtained for the hardening modulus rate h/τ^{22} as a function of the ratio $q = \dfrac{h_1}{h}$ are plotted in Fig. 18, and the misalignment angle δ as a function of the ratio q is shown in Fig. 19.

For nitrogenated Fe-Ti-Mn single crystals the orientation is as follows: $s_1 = (0,1,1)$, $m_1 = [1,\bar{1},1]$ and $s_2 = (1,0,1)$, $m_2 = [\bar{1},1,1]$. The numerical results obtained for the hardening modulus rate h/τ^{22} as a function of the ratio q are presented in Fig. 20, and for the misalignment angle δ as a function of the ratio q are plotted in Fig. 21.

The influence of the assumed value for the irreversibility coefficient χ on the inception of the adiabatic shear-band localization for Al-Cu single crystals is presented in Figs. 22 and 23.

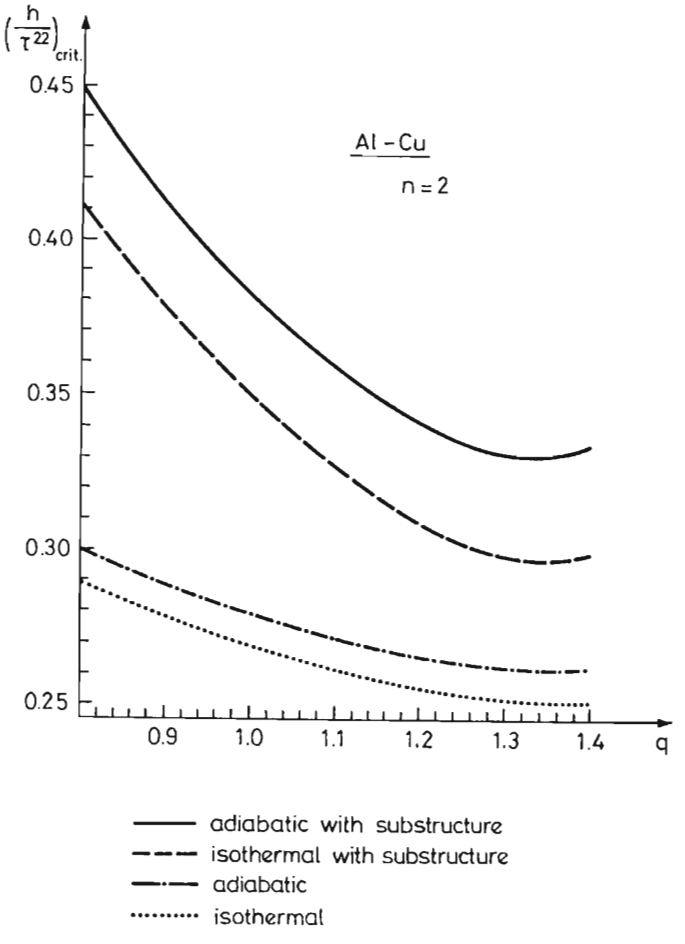

FIG. 18. Numerical results for symmetric double slip process for the hardening modulus rate h/τ^{22} as function of the ratio q for Al-Cu single crystal.

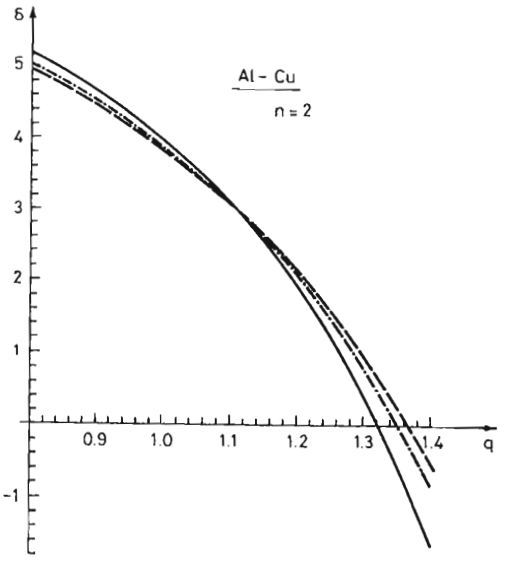

FIG. 19. Numerical results for symmetric double slip process for the misalignment angle δ as a function of the ratio q for Al-Cu single crystal.

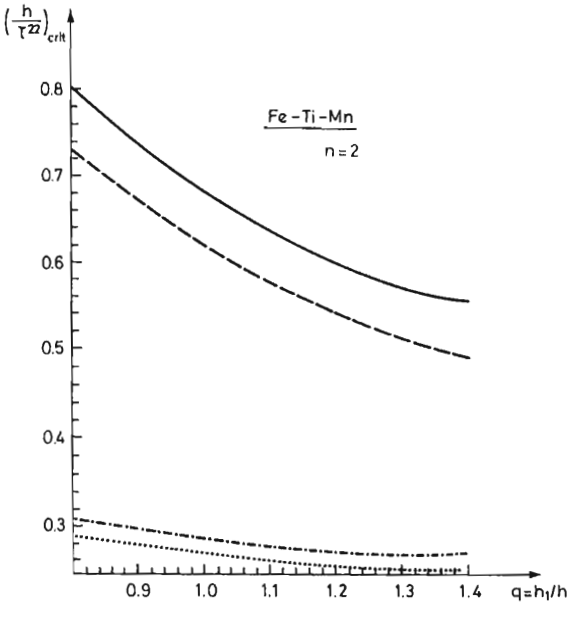

FIG. 20. Numerical results for symmetric double slip process for the hardening modulus rate h/τ^{22} as function of the ratio q for Fe-Ti-Mn single crystal.

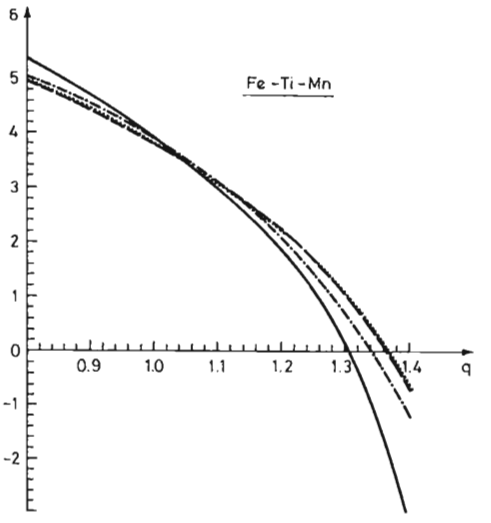

FIG. 21. Numerical results for symmetric double slip process for the misalignment angle δ as function of the ratio q for Fe-Ti-Mn single crystal.

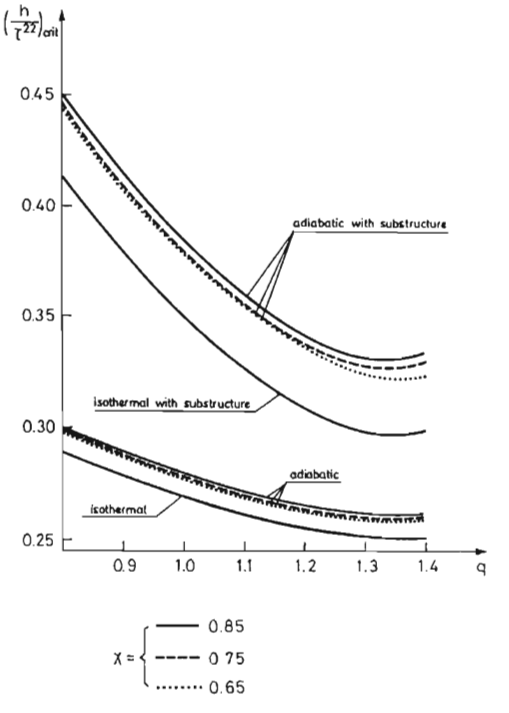

FIG. 22. The influence of the assumed value for the irreversibility coefficient χ on the hardening modulus rate h/τ^{22} for Al-Cu single crystal.

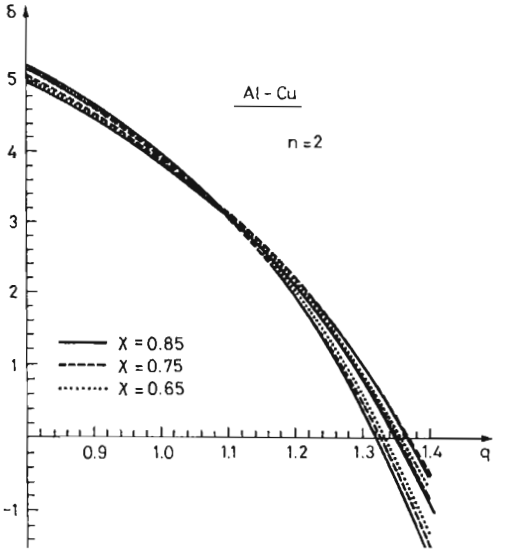

FIG. 23. The influence of the assumed value for the irreversibility coefficient χ on the misalignment angle δ for Al-Cu single crystal.

9.3. Discussion and comparison

Comparison of the analytical theoretical results with the available experimental observations of CHANG and ASARO [8] for aluminum-copper single crystals tested at 298 K, and SPITZIG [64] for nitrogenated Fe-Ti-Mn single crystals tested at 295 K, clearly shows that the influence of the dislocation substructure on the critical hardening modulus rate is very pronounced. However, the misalignment of the macroscopic shear-bands from the active slip systems in crystal's matrix is not very much affected by the influence of the evolution of substructure.

Comparison of the theoretical results plotted in Figs. 14–21 with those obtained experimentally by CHANG and ASARO [8] and SPITZIG [64] shows that the theoretical results for $\left(\frac{h}{\tau^{22}}\right)_{\text{crit}}$ give higher values. This seems to be natural since the experimental observations detected the values of the hardening modulus rate when the shear-band had been already well developed, while the theoretical predictions were computed at the inception of the shear-band localization.

Comparison of the theoretical results for the misalignment angle δ plotted in Figs. 19 and 21 with those obtained experimentally by CHANG and ASARO [8], LISIECKI *et al.* [35] and SPITZIG [64], shows that the theoretical predictions give good agreement.

It is noteworthy that different situation takes place for a single slip process when the geometry of the deformed specimen is simplified and the misalignment angle δ computed analytically is too small.

It should be pointed out that the influence of the evolution of the dislocation substructure is combined with the thermomechanical coupling and it gives a distinct synergetic effect. This synergetic effect is very well visible from the results presented in Figs. 18 and 20.

The changes of the assumed value for the irreversibility coefficient χ in the range of $0.65 - 0.85$ (as it has been suggested by Mason *et al.* [38]) does not influence the inception of the adiabatic shear-band localization too much, cf. Figs. 22 and 23.

10. Final comments

The main features of the theory of thermodynamic viscoplasticity of single crystals developed in this paper are as follows: (i) it is invariant under any diffeomorphism: (ii) it takes into considerations such important effects as thermomechanical coupling, the evolution of the dislocations substructure, the non-Schmid law, the spatial covariance and plastic spin; (iii) it describes cooperative phenomena and as the result, it takes account of synergetic effects.

To accomplish this purpose, the theory has been developed within the thermodynamic framework of the rate-type covariance constitutive structure with finite set of the internal state variables. The crucial idea in this theory is the very efficient physical interpretation of the internal state variables. Assumption that $\alpha^{(\nu)}$ and $\beta^{(\nu)}$ are interpreted as densities of mobile and obstacle dislocations in a particular slip system ν, respectively, and $\xi^{(\nu)}$ as the concentration of point defects, permitted to base all considerations on good physical foundations and to use the available experimental observations of single crystals.

This theory has been inspired by recent theoretical and experimental investigations by Follansbee [19], Rashid *et al.* [57], Asaro and Rice [3], Chang and Asaro [7, 8], Spitzig [64] and Lisiecki *et al.* [35]. All these mentioned works present deep understanding of real features of the deformation process of single crystals and have given many important measurements needed for the development of the theoretical descriptions.

The necessary criterion for the adiabatic shear-band localization introduced allows to discuss particular effects which can affect the localization phenomena in single slip, as well as in symmetric double slip processes. It has been proved that the cooperative phenomena play a very important role in the development of macroscopic shear-band localization of plastic deformation in single crystals.

Acknowledgment

The paper has been prepared partly within the research programme sponsored by the Committee of Scientific Research under Grant 7 T07 A006 16.

REFERENCES

1. R. ABRAHAM, J.E. MARSDEN and T. RATIU, *Manifolds, tensor analysis and applications*, Springer, Berlin 1988.
2. R.J. ASARO, *Micromechanics of crystals and polycrystals*, Adv. Appl. Mech., **23**, 1–115, 1983.
3. R.J. ASARO, J.R. RICE, *Strain localization in ductile single crystals*, J. Mech. Phys. Solids, **25**, 309–338, 1977.
4. H. BALKE, Y. ESTRIN, *Micromechanical modelling of shear-banding in single crystals*, Int. J. Plast., **10**, 133–147, 1994.
5. S.J. BASIŃSKI, Z.S. BASIŃSKI, *Plastic deformation and work hardening*, Dislocations in Solids, Vol.4 Dislocations in Metallurgy, F.R.N. NABARRO [Ed.], 261–362, Nort-Holland, Amsterdam 1979.
6. J.L. BASSANI, *Plastic flow of crystals*, Adv. Appl. Mech., **30**, 191–258, 1994.
7. Y.W. CHANG, R.J. ASARO, *Lattice rotations and shearing in crystals*, Arch. Mech., **32**, 369–388, 1980.
8. Y.W. CHANG, R.J. ASARO, *An experimental study of shear localization in aluminum-copper single crystals*, Acta Metall., **29**, 241–257, 1981.
9. B.D. COLEMAN, M.E. GURTIN, *Thermodynamics with internal state variables*, J. Chem. Phys., **47**, 597–613, 1967.
10. B.D. COLEMAN, W. NOLL, *The thermodynamics of elastic materials with heat conduction and viscosity*, Arch. Rational Mech. Anal., **13**, 167–178, 1963.
11. H. CONRAD, *Thermally activated deformation of metals*, J. Metals, **16**, 582–588, 1964.
12. W.A. DAY, M. SILHAVY, *Efficiency and the existence of entropy in classical thermodynamics*, Arch. Rational Mech. Anal., **64**, 205–219, 1977.
13. M.K. DUSZEK, P. PERZYNA, *The localization of plastic deformation in thermoplastic solids*, Int. J. Solids Structures, **27**, 1419–1443, 1991.
14. M.K. DUSZEK-PERZYNA, P. PERZYNA, *Adiabatic shear-band localization in elastic-plastic single crystals*, Int. J. Solids Structures, **30**, 61–89, 1993.
15. M.K. DUSZEK-PERZYNA, P. PERZYNA, *Adiabatic shear-band localization of inelastic single crystals in symmetric double slip process*, Archive of Appled Mechanics, **66**, 369–384, 1996.
16. M.K. DUSZEK-PERZYNA, P. PERZYNA and E. STEIN, *Adiabatic shear-band localization in elastic-plastic damaged solids*, Int. J. Plasticity, **8**, 361–384, 1992.
17. Y. ESTRIN, L.P. KUBIN, *Load strain hardening and nonuniformity of plastic deformation*, Acta Metall., **34**, 2455–2464, 1986.
18. A.G. EVANS , R.D. KUMBLE, *The thermally activated deformation of crystalline materials*, Phys. Stat. Sol., **34**, 9–31, 1969.
19. P.S. FOLLANSBEE, *Metallurgical applications of shock – wave and high-strain-rate phenomena*, L.E. MURR, K.P. STAUDHAMMER, M.A. MEYERES [Eds.], 451–480, Marcel Dekker, New York 1986.

20. P.S. FOLLANSBEE, U.F. KOCKS, *A constitutive description of the deformation of copper based on the use of the mechanical threshold stress as an internal state variable*, Acta Met., **36**, 81–93, 1988.

21. P. GLANSDORFF, I. PRIGOGINE, *Thermodynamic theory of structure, stability and fluctuations*, Wiley-Interscience, London 1977.

22. J.A. GORMAN, D.S. WOOD and T. VREELAND, *Mobility of dislocation in aluminium*, J. Appl. Phys., **40**, 833–841, 1969.

23. A.E. GREEN, P.M. NAGHDI, *On thermodynamics and the nature of the second law*, Proc. R. Soc. Lond., **A357**, 253–270, 1977.

24. A.E. GREEN, P.M. NAGHDI, *On thermodynamics and the nature of the second law for mixtures of interacting continua*, Quart. J. Mech. Appl. Maths., **31**, 265–293, 1978.

25. M.E. GURTIN, *Thermodynamics and stability*, Arch. Rational Mech. Anal., **59**, 63–96, 1975.

26. J. HADAMARD, *Lecons sur la propagation des ondes et les equations de l'hydrodynamique*, Chap. 6, Paris 1903.

27. H. HAKEN, *Cooperative phenomena in systems far from thermal equilibrium and in non-physical systems*, Reviews of Modern Physics, **47**, 67–121, 1975.

28. H. HAKEN, *Advanced Synergetics*, Springer, Berlin 1987.

29. H. HAKEN, *Information and self-organization*, Springer, Berlin 1988.

30. R. HILL, *Acceleration wave in solids*, J. Mech. Phys. Solids, **10**, 1–16, 1962.

31. R. HILL, J.R. RICE, *Constitutive analysis of elastic-plastic crystals at arbitrary strain*, J. Mech. Phys. Solids, **20**, 401–413, 1972.

32. G. JAUMANN, *Geschlossenes System physikalischer und chemischer Differentialgesetze*, Sitzungsber. Akad. Wiss. Wien (IIa), **120**, 385–530, 1911.

33. U.F. KOCKS, A.S. ARGON and M.F. ASHBY, *Thermodynamics and kinetics of slip*, Pergamon Press, 1975.

34. A. KUMAR, R.G. KUMBLE, *Viscous drag on dislocations at high strain-rates in copper*, J. Appl. Physics, **40**, 3475–3480, 1969.

35. L.L. LISIECKI, D.R. NELSON and R.J. ASARO, *Lattice rotations, necking and localized deformation in f.c.c. single crystals*, Scripta Met., **16**, 441–449, 1982.

36. J.E. MARSDEN, T.J.R. HUGHES, *Mathematical foundations of elasticity*, Prentice-Hall, Englewood Cliffs, New York 1983.

37. W.P. MASON, *Phonon viscosity and its effect on acoustic wave attenuation and dislocation motion*, J. Acoustical Soc. Amer., **32**, 458–472, 1960.

38. J.J. MASON, A.J. ROSAKIS and R. RAVICHANDRAN, *On the strain and strain-rate dependence of the fraction of plastic work converted to heat: an experimental study using high speed infrared detectors and the Kolsky bar*, Mechanics of Materials, **17**, 135–145, 1994.

39. H. MECKING, U.F. KOCKS, *Kinetics of flow and strain-hardening*, Acta Metall., **29**, 1865–1875, 1981.

40. I. MÜLLER, *On the entropy inequality*, Arch. Rational Mech. Anal., **26**, 118–141, 1967.

41. I. MÜLLER, *Thermodynamics of mixtures of fluids*, J. Mécanique, **14**, 267–303, 1975.

42. F.N.R. NABARRO, *Theory of crystal dislocations*, Oxford 1967.

43. S. NEMAT-NASSER, *Phenomenological theories of elastoplasticity and strain localization at high strain-rates*, Appl. Mech. Rev., **45**, S19–S45, 1992.

44. G. NICOLIS, I. PRIGOGINE, *Self-organization in nonequilibrium systems*, Wiley-Interscience, New York 1977.

45. J. OLDROYD, *On the formulation of rheological equations of state*, Proc. R. Soc. Lond., **A200**, 523–541, 1950.

46. D. PEIRCE, J.R. ASARO and A. NEEDLEMAN, *An analysis of nonuniform and localized deformation in ductile single crystals*, Acta Metall., **30**, 1087–1119, 1982.

47. D. PEIRCE, J.R. ASARO and A. NEEDLEMAN, *Material rate dependence and localized deformation in crystalline solids*, Acta Metall., **31**, 1951–1976, 1983.

48. P. PERZYNA, *Coupling of dissipative mechanisms of viscoplastic flow*, Arch. Mechanics, **29**, 607–624, 1977.

49. P. PERZYNA, *Temperature and rate-dependent theory of plasticity of crystalline solids*, Revue Phys. Appl., **23**, 445–459, 1988.

50. P. PERZYNA, *Instability phenomena and adiabatic shear-band localization in thermoplastic flow processes*, Acta Mechanica, **106**, 173–205, 1994.

51. P. PERZYNA, *Thermodynamics of crystal viscoplasticity and instability phenomena*, Material Instability in Solids, (R. de Borst, E. van Giessen, [Eds.]), 65–89, John Wiley and Sons, New York 1998.

52. P. PERZYNA, M.K. DUSZEK-PERZYNA, *Constitutive modelling of inelastic single crystals for localization phenomena*, Constitutive Laws: Experiments and Numerical Implementation, A.M. RAJENDRAN, R.C. BATRA [Eds.], 70–83., CIMME, Barcelona 1995.

53. P. PERZYNA, K. KORBEL, *Analysis of the influence of substructure of crystal on the localization phenomena of plastic deformation*, Mechanics of Materials, **24**, 141–158, 1996.

54. P. PERZYNA, K. KORBEL, *Analysis of the influence of variuos effects on criteria for adiabatic shear-band localization in single crystals*, Acta Mechanica, **129**, 31–62, 1998.

55. Q. QIN, J.L. BASSANI, *Non-Schmid yield behavior in single crystals*, J. Mech. Phys. Solids, **40**, 813–833, 1992.

56. Q. QIN, J.L. BASSANI, *Non-associated plastic flow in single crystals*, J. Mech. Phys. Solids, **40**, 835–862, 1992.

57. M.M. RASHID, G.T. GRAY and S. NEMAT-NASSER, *Heterogeneous deformations n copper single crystals at high and low strain-rates*, Philosophical Magazine A, **65**, 707–735, 1992.

58. J.R. RICE, *The localization of plastic deformation*, Theoretical and Applied Mechanics, W.T. KOITER [Ed.], 207–220. North-Holand, 1976.

59. J.W. RUDNICKI, J.R. RICE, *Conditions for the localization of deformation in pressure-sensitive dilatant materials*, J. Mech. Phys. Solids, **23**, 371–394, 1975.

60. A. SEEGER, *The generation of lattice defects by moving dislocations and its application to the temperature dependence of the flow-stress of f.c.c. crystals*, Phil. Mag., **46**, 1194–1217, 1955.

61. A. SEEGER, *Kristalplastizitat*, Handbuch der Physik VII/2, S. FLÜGGE [Ed.], 1–208, Springer-Verlag, 1958.

62. J. SERRIN,, *Conceptual analysis of the classical second laws of thermodynamics*, Arch. Rational Mech. Anal., **70**, 355–371, 1979.

63. I.S. SOKOLNIKOFF, *The mathematical theory of elasticity*, (2nd. ed.), Mc Graw-Hill, New York 1956.

64. W.A. SPITZIG, *Deformation behaviour of nitrogenated Fe-Ti-Mn and Fe-Ti single crystals*, Acta Metall., **29**, 1359–1377, 1981.

65. G.I. TAYLOR, *Analysis of plastic strain in a crystal*, Stephen Timoshenko 60th Anniversary Volume, J.M. LESSELS [Ed.], MacMillan, New York 1938.

66. G.I. TAYLOR, H. QUINNEY, *The latent energy remaining in a metal after cold working*, Proc. R. Soc. Lond., **A143**, 307–326, 1934.

67. C. TEODOSIU, F. SIDOROFF, *A theory of finite elastoplasticity of single crystals*, Int. J. Engng. Sci., **14**, 165–176, 1976.

68. C. TRUESDELL, *Rational Thermodynamics*, Mc Graw-Hill, New York 1969.

69. C. TRUESDELL, W. NOLL, *The non-linear field theories of mechanics*, Handbuch der Physik III/3, S. FLÜGGE [Ed.], Springer-Verlag, Berlin 1965.

70. J.C. WILLEMS, *Dissipative dynamical systems*, Arch. Rat. Mech. Anal., **45**, 321–393, 1972.

71. S. ZAREMBA, *Sur une forme perfectionnée de la théorie de la relaxation*, Bull. Int. Acad. Sci. Cracovie, 594–614, 1903.

72. S. ZAREMBA, *Le principe des mouvements relatifs et les équations de la mécanique physique*, Bull. Int. Acad. Sci. Cracovie, 614–621, 1903.

Received October 24, 2001; revised version March 1, 2002.